Molecular cloning and bacterial expression of cDNA encoding a plant cysteine synthase. Proc. Natl. Acad. Sci. USA 89:8078–8082.

271. **Saito, K., K. Tatsuguchi, I. Murakoshi, and H. Hirano.** 1993. cDNA cloning and expression of cysteine synthase B localized in chloroplasts of *Spinacia oleracea*. FEBS Lett. 324:247–252.
272. **Saito, K., K. Tatsuguchi, Y. Takagi, and I. Murakoshi.** 1994. Isolation and characterization of cDNA that encodes a putative mitochondrion-localizing isoform of cysteine synthase (*O*-acetylserine(thiol)-lyase) from *Spinacia oleracea*. J. Biol. Chem. 269:28187–28192.
273. **Saito, K., H. Yokoyama, M. Noji, and I. Murakoshi.** 1995. Molecular cloning and characterization of a plant serine acetyltransferase playing a regulatory role in cysteine biosynthesis from watermelon. J. Biol. Chem. 270: 16321–16326.
274. **Samarawickrema, N. A., D. M. Brown, J. A. Upcroft, N. Thammapalerd, and P. Upcroft.** 1997. Involvement of superoxide dismutase and pyruvate: ferredoxin oxidoreductase in mechanisms of metronidazole resistance in *Entamoeba histolytica*. J. Antimicrob. Chemother. 40:833–840.
275. **Samuelson, J.** 1999. Why metronidazole is active against both bacteria and parasites. Antimicrob. Agents Chemother. 43:1533–1541.
276. **Samuelson, J., P. Ayala, E. Orozco, and D. Wirth.** 1990. Emetine-resistant mutants of *Entamoeba histolytica* overexpress mRNAs for multidrug resistance. Mol. Biochem. Parasitol. 38:281–290.
277. **Samuelson, J. C., A. Burke, and J. M. Courval.** 1992. Susceptibility of an emetine-resistant mutant of *Entamoeba histolytica* to multiple drugs and to channel blockers. Antimicrob. Agents Chemother. 36:2392–2397.
278. **Sanchez, L., V. Enea, and D. Eichinger.** 1994. Identification of a developmentally regulated transcript expressed during encystation of *Entamoeba invadens*. Mol. Biochem. Parasitol. 67:125–135.
279. **Saurina, G. R., and W. M. McCormack.** 1997. Trichomoniasis in pregnancy. Sex. Transm. Dis. 24:361–362.
280. **Savioli, L., H. Smith, and A. Thompson.** 2006. *Giardia* and *Cryptosporidium* join the 'Neglected Diseases Initiative'. Trends Parasitol. 22:203–208.
281. **Schwebke, J. R., T. Aira, N. Jordan, P. E. Jolly, and S. H. Vermund.** 1998. Sexually transmitted diseases in Ulaanbaatar, Mongolia. Int. J. STD AIDS 9:354–358.
282. **Schwebke, J. R., and D. Burgess.** 2004 Trichomoniasis. Clin. Microbiol. Rev. 17:794–803.
283. **Schwebke, J. R., and E. W. Hook III.** 2003. High rates of *Trichomonas vaginalis* among men attending a sexually transmitted diseases clinic: implications for screening and urethritis management. J. Infect. Dis. 188:465–468.
284. **Seeber, F.** 2002. Biogenesis of iron-sulphur clusters in amitochondriate and apicomplexan protists. Int. J. Parasitol. 32:1207–1217.
285. **Sener, K., Z. Shen, D. S. Newburg, and E. L. Jarroll.** 2004. Amino sugar phosphate levels in *Giardia* change during cyst wall formation. Microbiology 150:1225–1230.
286. **Simjee, A. E., V. Gathiram, T. F. Jackson, and B. F. Khan.** 1985. A comparative trial of metronidazole v. tinidazole in the treatment of amoebic liver abscess. S. Afr. Med. J. 68:923–924.
287. **Singh, S., K. Husain, F. Athar, and A. Azam.** 2005. Synthesis and antiamoebic activity of 3,7-dimethyl-pyrazolo[3,4-e][1,2,4] triazin-4-yl thiosemicarbazide derivatives. Eur. J. Pharm. Sci. 25:255–262.
288. **Slamovits, C. H., and P. J. Keeling.** 2006. Pyruvate-phosphate dikinase of oxymonads and parabasalia and the evolution of pyrophosphate-dependent glycolysis in anaerobic eukaryotes. Eukaryot. Cell 5:148–154.
289. **Sobel, J. D., V. Nagappan, and P. Nyirjesy.** 1999. Metronidazole-resistant vaginal trichomoniasis—an emerging problem. N. Engl. J. Med. 341:292–293.
290. **Sobel, J. D., P. Nyirjesy, and W. Brown.** 2001. Tinidazole therapy for metronidazole-resistant vaginal trichomoniasis. Clin. Infect. Dis. 33:1341–1346.
291. **Sonda, S., and A. B. Hehl.** 2006. Lipid biology of Apicomplexa: perspectives for new drug targets, particularly for *Toxoplasma gondii*. Trends Parasitol. 22:41–47.
292. **Sorvillo, F., and P. Kerndt.** 1998. *Trichomonas vaginalis* and amplification of HIV-1 transmission. Lancet 351:213–214.
293. **Stanley, S. L., Jr.** 2003 Amoebiasis. Lancet 361:1025–1034.
294. **Sutak, R., P. Dolezal, H. L. Fiumera, I. Hrdy, A. Dancis, M. Delgadillo-Correa, P. J. Johnson, M. Muller, and J. Tachezy.** 2004. Mitochondrial-type assembly of FeS centers in the hydrogenosomes of the amitochondriate eukaryote *Trichomonas vaginalis*. Proc. Natl. Acad. Sci. USA 101:10368–10373.
295. **Tachezy, J., L. B. Sanchez, and M. Muller.** 2001. Mitochondrial type iron-sulfur cluster assembly in the amitochondriate eukaryotes *Trichomonas vaginalis* and *Giardia intestinalis*, as indicated by the phylogeny of IscS. Mol. Biol. Evol. 18:1919–1928.
296. **Takeuchi, T., E. C. Weinbach, M. Gottlieb, and L. S. Diamond.** 1979. Mechanism of L-serine oxidation in *Entamoeba histolytica*. Comp. Biochem. Physiol. B 62:281–285.
297. **Tannich, E., I. Bruchhaus, R. D. Walter, and R. D. Horstmann.** 1991. Pathogenic and nonpathogenic *Entamoeba histolytica*: identification and molecular cloning of an iron-containing superoxide dismutase. Mol. Biochem. Parasitol. 49:61–71.
298. **Terai, K., T. Masuda, and H. Miyamoto.** 1999. Survey of amebiasis at an institution for the mentally retarded in Shizuoka Prefecture. Kansenshogaku Zasshi 73:626–627.
299. **Thong, K. W., G. H. Coombs, and B. E. Sanderson.** 1987. L-Methionine catabolism in trichomonads. Mol. Biochem. Parasitol. 23:223–231.
300. Reference deleted.
301. **Tokoro, M., T. Asai, S. Kobayashi, T. Takeuchi, and T. Nozaki.** 2003. Identification and characterization of two isoenzymes of methionine gamma-lyase from *Entamoeba histolytica*: a key enzyme of sulfur-amino acid degradation in an anaerobic parasitic protist that lacks forward and reverse transsulfuration pathways. J. Biol. Chem. 278:42717–42727.
302. **Tokumoto, U., S. Kitamura, K. Fukuyama, and Y. Takahashi.** 2004. Interchangeability and distinct properties of bacterial Fe-S cluster assembly systems: functional replacement of the isc and suf operons in *Escherichia coli* with the nifSU-like operon from *Helicobacter pylori*. J. Biochem. (Tokyo) 136:199–209.
303. **Tovar, J., A. Fischer, and C. G. Clark.** 1999. The mitosome, a novel organelle related to mitochondria in the amitochondrial parasite *Entamoeba histolytica*. Mol. Microbiol. 32:1013–1021.
304. **Tovar, J., G. Leon-Avila, L. B. Sanchez, R. Sutak, J. Tachezy, M. Van Der Giezen, M. Hernandez, M. Muller, and J. M. Lucocq.** 2003. Mitochondrial remnant organelles of *Giardia* function in iron-sulphur protein maturation. Nature 426:172–176.
305. **Townsend, D. M., K. D. Tew, and H. Tapiero.** 2004. Sulfur containing amino acids and human disease. Biomed. Pharmacother. 58:47–55.
306. **Townson, S. M., P. F. Boreham, P. Upcroft, and J. A. Upcroft.** 1994. Resistance to the nitroheterocyclic drugs. Acta Trop. 56:173–194.
307. **Townson, S. M., G. R. Hanson, J. A. Upcroft, and P. Upcroft.** 1994. A purified ferredoxin from *Giardia duodenalis*. Eur. J. Biochem. 220:439–446.
308. **Townson, S. M., J. A. Upcroft, and P. Upcroft.** 1996. Characterisation and purification of pyruvate:ferredoxin oxidoreductase from *Giardia duodenalis*. Mol. Biochem. Parasitol. 79:183–193.
309. **Upcroft, J., R. Mitchell, N. Chen, and P. Upcroft.** 1996. Albendazole resistance in *Giardia* is correlated with cytoskeletal changes but not with a mutation at amino acid 200 in beta-tubulin. Microb. Drug Resist. 2:303–308.
310. **Upcroft, J. A., R. W. Campbell, K. Benakli, P. Upcroft, and P. Vanelle.** 1999. Efficacy of new 5-nitroimidazoles against metronidazole-susceptible and -resistant *Giardia*, *Trichomonas*, and *Entamoeba* spp. Antimicrob. Agents Chemother. 43:73–76.
311. **Upcroft, J. A., R. W. Campbell, and P. Upcroft.** 1996 Quinacrine-resistant *Giardia duodenalis*. Parasitology 112:309–313.
312. **Upcroft, J. A., and P. Upcroft.** 1993. Drug resistance and *Giardia*. Parasitol. Today 9:187–190.
313. **Upcroft, J. A., and P. Upcroft.** 1999. Keto-acid oxidoreductases in the anaerobic protozoa. J. Eukaryot. Microbiol. 46:447–449.
314. **Upcroft, P., and J. A. Upcroft.** 2001. Drug targets and mechanisms of resistance in the anaerobic protozoa. Clin. Microbiol. Rev. 14:150–164.
315. **van der Giezen, M., S. Cox, and J. Tovar.** 2004. The iron-sulfur cluster assembly genes iscS and iscU of *Entamoeba histolytica* were acquired by horizontal gene transfer. BMC Evol. Biol. 4:7.
316. **van der Giezen, M., J. Tovar, and C. G. Clark.** 2005. Mitochondrion-derived organelles in protists and fungi. Int. Rev. Cytol. 244:175–225.
317. **Vazquezdelara-Cisneros, L. G., and A. Arroyo-Begovich.** 1984. Induction of encystation of *Entamoeba invadens* by removal of glucose from the culture medium. J. Parasitol. 70:629–633.
318. **Verhagen, M. F., T. O'Rourke, and M. W. Adams.** 1999. The hyperthermophilic bacterium, *Thermotoga maritima*, contains an unusually complex iron-hydrogenase: amino acid sequence analyses versus biochemical characterization. Biochim. Biophys. Acta 1412:212–229.
319. **Voolmann, T., and P. Boreham.** 1993. Metronidazole resistant *Trichomonas vaginalis* in Brisbane. Med. J. Aust. 159:490.
320. **Wallis, P. M.** 1994. Abiotic transmission—is water really significant?, p. 99–122. *In* R. C. A. Thompson, J. A. Reynoldson, and A. J. Lymberg (ed.), *Giardia*: from molecules to disease. CAB International, Wallingford, United Kingdom.
321. **Walsh, J. A.** 1986. Problems in recognition and diagnosis of amebiasis: estimation of the global magnitude of morbidity and mortality. Rev. Infect. Dis. 8:228–238.
322. **Wang, C. C., R. Verham, S. F. Tzeng, S. Aldritt, and H. W. Cheng.** 1983. Pyrimidine metabolism in *Tritrichomonas foetus*. Proc. Natl. Acad. Sci. USA 80:2564–2568.
323. **Wassmann, C., A. Hellberg, E. Tannich, and I. Bruchhaus.** 1999. Metronidazole resistance in the protozoan parasite *Entamoeba histolytica* is associated with increased expression of iron-containing superoxide dismutase and peroxiredoxin and decreased expression of ferredoxin 1 and flavin reductase. J. Biol. Chem. 274:26051–26056.
324. **Weber, G., W. Mohr, K. Fleischer, and P. G. Sargeaunt.** 1990. *Entamoeba histolytica* infections in flight personnel of an international airline. Trans. R. Soc. Trop. Med. Hyg. 84:803–805.

325. **Weinbach, E. C., and L. S. Diamond.** 1974. *Entamoeba histolytica*. I. Aerobic metabolism. Exp. Parasitol. **35**:232–243.
326. **Westrop, G. D., G. Goodall, J. C. Mottram, and G. H. Coombs.** 2006. Cysteine biosynthesis in *Trichomonas vaginalis* involves cysteine synthase utilizing *O*-phosphoserine. J. Biol. Chem. **281**:25062–25075.
327. **Whiteway, J., P. Koziarz, J. Veall, N. Sandhu, P. Kumar, B. Hoecher, and I. B. Lambert.** 1998. Oxygen-insensitive nitroreductases: analysis of the roles of *nfsA* and *nfsB* in development of resistance to 5-nitrofuran derivatives in *Escherichia coli*. J. Bacteriol. **180**:5529–5539.
328. Reference deleted.
329. **Wiesner, J., and F. Seeber.** 2005. The plastid-derived organelle of protozoan human parasites as a target of established and emerging drugs. Expert Opin. Ther. Targets **9**:23–44.
330. **Williams, K., P. N. Lowe, and P. F. Leadlay.** 1987. Purification and characterization of pyruvate:ferredoxin oxidoreductase from the anaerobic protozoon *Trichomonas vaginalis*. Biochem. J. **246**:529–536.
331. **Wilson, R. J., K. Rangachari, J. W. Saldanha, L. Rickman, R. S. Buxton, and J. F. Eccleston.** 2003. Parasite plastids: maintenance and functions. Philos. Trans. R. Soc. London B **358**:155–164.
332. **Wirtz, M., O. Berkowitz, M. Droux, and R. Hell.** 2001. The cysteine synthase complex from plants. Mitochondrial serine acetyltransferase from *Arabidopsis thaliana* carries a bifunctional domain for catalysis and protein-protein interaction. Eur. J. Biochem. **268**:686–693.
333. **World Health Organization.** 1998. Intestinal parasites control: burden and trends. World Health Organization, Geneva, Switzerland.
334. **Yarlett, N., H. Hof, and N. C. Yarlett.** 1987. Activities of metronidazole and niridazole against *Trichomonas vaginalis* clinical isolates. J. Antimicrob. Chemother. **19**:767–770.
335. **Yarlett, N., C. C. Rowlands, N. C. Yarlett, J. C. Evans, and D. Lloyd.** 1987. Reduction of niridazole by metronidazole resistant and susceptible strains of *Trichomonas vaginalis*. Parasitology **94**:93–99.
336. **Yarlett, N., N. C. Yarlett, and D. Lloyd.** 1986. Metronidazole-resistant clinical isolates of *Trichomonas vaginalis* have lowered oxygen affinities. Mol. Biochem. Parasitol. **19**:111–116.
337. **Yong, T. S., E. Li, D. Clark, and S. L. Stanley, Jr.** 1996. Complementation of an *Escherichia coli* adhE mutant by the *Entamoeba histolytica* EhADH2 gene provides a method for the identification of new antiamebic drugs. Proc. Natl. Acad. Sci. USA **93**:6464–6469.
338. **Yoshimura, M., Y. Nakano, and T. Koga.** 2002. L-Methionine-gamma-lyase, as a target to inhibit malodorous bacterial growth by trifluoromethionine. Biochem. Biophys. Res. Commun. **292**:964–968.
339. **Zaat, J. O., T. G. Mank, and W. J. Assendelft.** 1997. A systematic review on the treatment of giardiasis. Trop. Med. Int. Health **2**:63–82.
340. **Zhang, Y. Q., Z. Y. Wang, S. Q. Lu, M. L. Feng, J. F. Peng, and J. G. Wang.** 1986. A familial infection of giardiasis. Chin. Med. J. **99**:417–419.
341. **Zhong, H. L., W. J. Cao, J. F. Rossignol, M. L. Feng, R. Y. Hu, S. B. Gan, and W. Tan.** 1986. Albendazole in nematode, cestode, trematode and protozoan (*Giardia*) infections. Chin. Med. J. **99**:912–915.
342. **Zygmunt, W. A., and P. A. Tavormina.** 1966. DL-S-Trifluoromethylhomocysteine, a novel inhibitor of microbial growth. Can. J. Microbiol. **12**:143–148.

Cellular Microbiology (2007) 9(7), 1796–1808

doi:10.1111/j.1462-5822.2007.00915.x
First published online 13 March 2007

Two Rab7 isotypes, *Eh*Rab7A and *Eh*Rab7B, play distinct roles in biogenesis of lysosomes and phagosomes in the enteric protozoan parasite *Entamoeba histolytica*

Yumiko Saito-Nakano,[1] Biswa Nath Mitra,[2] Kumiko Nakada-Tsukui,[2] Dan Sato[2] and Tomoyoshi Nozaki[2]*

[1]*Department of Parasitology, National Institute of Infectious Diseases, 1-23-1 Toyama, Shinjuku-ku, Tokyo 162-8640, Japan.*

[2]*Department of Parasitology, Gunma University Graduate School of Medicine, 3-39-22 Showa-machi, Maebashi, Gunma 371-8511, Japan.*

Summary

Rab7 small GTPase plays a crucial role in the regulation of trafficking to late endosomes, lysosomes and phagosomes. While most eukaryotes encode a single Rab7, the parasitic protist *Entamoeba histolytica* possesses nine Rab7. In this study, to understand the significance of the presence of multiple Rab7 isotypes, a role of two representative Rab7 isotypes, *Eh*Rab7A and *Eh*Rab7B, was investigated. *Eh*Rab7B was exclusively localized to acidic vacuoles containing lysosomal proteins, e.g. amoebapore-A and cysteine protease. This lysosome localization of *Eh*Rab7B was in good contrast to *Eh*Rab7A, localized to a non-acidic compartment in steady state, and only partially colocalized with lysosomal proteins. Overexpression of *Eh*Rab7B resulted in augmentation of late endosome/lysosome acidification, similar to the *Eh*Rab7A overexpression. Expression of *Eh*Rab7B-GTP mutant caused dominant-negative phenotypes including decrease in late endosome/lysosome acidification and missecretion of lysosomal proteins, while *Eh*Rab7A-GTP enhanced acidification but did not affect either intracellular or secreted cysteine protease activity. Expression of either *Eh*Rab7B or *Eh*Rab7B-GTP mutant caused defect in phagocytosis, concomitant with the disturbed formation and disassembly of prephagosomal vacuoles, the compartment previously shown to be linked to efficient ingestion. Altogether, these data indicate that the two Rab7 isotypes play distinct but co-ordinated roles in lysosome and phagosome biogenesis.

Received 9 November, 2006; revised 24 January, 2007; accepted 30 January, 2007. *For correspondence. E-mail nozaki@med.gunma-u.ac.jp; Tel. (+81) 27 2208020; Fax (+81) 27 2208025.

Introduction

Lysosomes serve as a compartment to degrade endocytosed materials with various hydrolytic and degradative proteins. Lysosomes also play a role as a compartment to process, activate and store proteins secreted extracellularly (Mullins and Bonifacino, 2001; Bowers and Stevens, 2005). Among a number of molecules involved in the lysosome biogenesis, one of the most important players is Rab7 small GTPase (Mullins and Bonifacino, 2001). Roles of Rab7 are significantly divergent between organisms and cell types; Rab7 plays a role on several distinct steps of endosomal or lysosomal trafficking (Feng *et al.*, 1995; Meresse *et al.*, 1995; Vitelli *et al.*, 1997; Bucci *et al.*, 2000). In baby hamster kidney cells, Rab7 was shown to mediate the early-to-late endosomal transport (Feng *et al.*, 1995; Vitelli *et al.*, 1997), whereas in HeLa cells, Rab7 was mainly associated with lysosomes and involved in lysosome acidification and transport of lysosomal proteins, but not of late endosomal proteins (Meresse *et al.*, 1995; Bucci *et al.*, 2000). Moreover, Rab7 was also shown to be required for fusion of late endosomes and lysosomes with primary phagosomes in professional phagocytes (Vieira *et al.*, 2003). In yeast, Ypt7p, the yeast Rab7 homologue, was also shown to be involved in transport from the late endosomes to the central vacuole, the yeast lysosome equivalent, and to be required for homotypic fusion of the vacuoles (Wichmann *et al.*, 1992; Schimmoller and Riezman, 1993; Haas *et al.*, 1995).

While many uni- and multicellular eukaryotes including *Saccharomyces cerevisiae*, *Trypanosoma brucei*, *Plasmodium falciparum*, *Caenorhabditis elegans*, *Drosophila melanogaster*, human, encode a single Rab7 (Pereira-Leal and Seabra, 2001; Quevillon *et al.*, 2003; Ackers *et al.*, 2005; Berriman *et al.*, 2005), some protozoan parasites including *Trichomonas vaginalis* and *Entamoeba histolytica* have three to nine Rab7 isotypes (Lal *et al.*, 2005; Saito-Nakano *et al.*, 2005), which is similar to plants such as *Lotus japonicus* and *Arabidopsis thaliana*, having four

to eight Rab7 isotypes (Borg *et al.*, 1997; Pereira-Leal and Seabra, 2001). In *L. japonicus*, some of Rab7 isotypes were expressed in a tissue-specific manner (Borg *et al.*, 1997), and also in *A. thaliana*, one of Rab7 isotypes was expressed tissue-specifically and its expression was induced by stress (Mazel *et al.*, 2004). However, the functional differences between Rab7 isotypes and biological significance of the redundancy in a unicellular organism have not been elucidated.

The unicellular enteric protist *E. histolytica* causes an estimated 50 million cases of amoebic dysentery, colitis and liver abscess in human, which leads to 100 000 deaths annually (Haque *et al.*, 2003; Huston, 2004). Among several factors including galactose/N-acetylgalactosamine (Gal/GalNAc)-inhibitable lectin (Vines *et al.*, 1998), the membranolytic peptide amoebapore (AP) (Leippe, 1999), and lysosomal hydrolase cysteine proteases (CP) (Que *et al.*, 2002) implicated for the multifactorial virulence mechanisms of *E. histolytica*, CPs are considered to be largely attributed to the pathogenesis of the parasite. Therefore, lysosome biogenesis that controls transport, maturation and secretion of CPs likely plays an important role in pathogenesis as well as housekeeping functions unrelated to parasitism and virulence in this organism (Nozaki and Nakada-Tsukui, 2006). *E. histolytica* has the largest number (96–106) of Rab GTPases, including nine of Rab7 isotypes, among organisms whose genome sequences are available (Welter *et al.*, 2002; Lal *et al.*, 2005; Saito-Nakano *et al.*, 2005). We have previously shown that one of Rab7 isotypes, *Eh*Rab7A, is involved in the transport of CPs, e.g. CP2, and AP to phagosomes via prephagosomal vacuoles (PPV), which are formed accompanied with phagocytosis, and likely serves to process, activate and store these lysosomal proteins prior to targeting to phagosomes (Saito-Nakano *et al.*, 2004). *Eh*Rab7A also regulates recycling of a CP receptor from phagosomes to the *trans*-Golgi network via interaction with the retromer-like complex (Nakada-Tsukui *et al.*, 2005; Nozaki and Nakada-Tsukui, 2006). However, a role of other Rab7 isotypes has not been elucidated. In this report, we describe that two Rab7 isotypes, *Eh*Rab7A and *Eh*Rab7B, play distinct but co-ordinated roles in lysosome biogenesis. To our knowledge, this is the first demonstration of distinct roles of Rab7 isotypes in lysosome and phagosomal biogenesis of unicellular organisms.

Results

All nine Eh*Rab7 isotypes are expressed under axenic culture conditions*

Entamoeba histolytica encodes nine Rab7 isotypes, designated as *Eh*Rab7A to *Eh*Rab7I (Saito-Nakano *et al.*, 2005), which is in marked contrast to mammals and yeasts, where only one Rab7/Ypt7p is encoded. These Rab7 isotypes showed 40–64% mutual identities and 32–56% identities to Rab7/Ypt7 homologues in other organisms, and designated alphabetically in a descending order of percentage identity to human Rab7 or yeast Ypt7. To validate that these Rab7 isotypes are transcribed, we measured the steady-state level of their transcripts under the axenic culture conditions. Quantitative real-time PCR (RT-PCR) showed that all nine *Eh*Rab7 isotypes are expressed above the measurable level, verifying that none of these *Eh*Rab7 genes is a pseudogene (Fig. 1). Six isotypes, i.e. *Eh*Rab7A, B, D, E, G and H, are expressed at the level of 0.3–3-fold of RNA polymerase II 15 kDa subunit while the three other isotypes were expressed at the lower level. The steady-state level of transcripts of *Eh*Rab7F and I was very low but reproducibly detectable (3.8% and 5.3% of RNA polymerase II 15 kDa subunit respectively). As *Eh*Rab7B, previously referred as 'a homologue of *Dictyostelium* Rab7D', was shown to be upregulated in the amoebae derived from an infected animal (Bruchhaus *et al.*, 2002), we also measured the level of steady-state transcripts of *Eh*Rab7 isotypes in the animal liver-derived highly virulent HM1 strain (Mitra *et al.*, 2006). However, all *Eh*Rab7 isotypes including *Eh*Rab7B remained unchanged upon the animal infection (data not shown). This result is consistent with our previous data showing that the amount of *Eh*Rab7 isotypes associated with phagosomes were comparable between axenically cultured avirulent and animal-passaged highly virulent strains (Okada *et al.*, 2006). In this work, we describe characterization of *Eh*Rab7A and *Eh*Rab7B, and studies on the other *Eh*Rab7 isotypes will be described elsewhere.

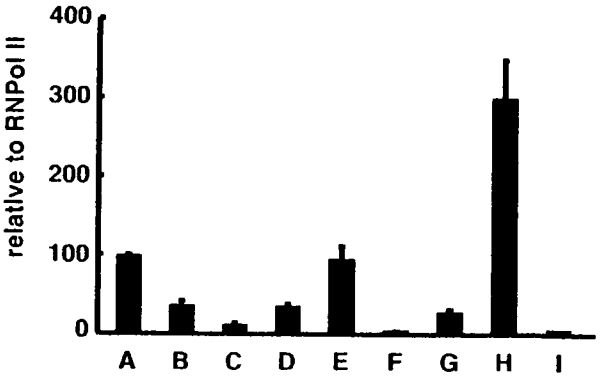

Fig. 1. Expression of nine *Eh*Rab7 isotypes under standard axenic culture conditions. The quantitative RT-PCR was performed using mRNA from the amoeba trophozoites cultivated axenically, and the amount of mRNAs of each isotype was normalized relative to the amount of RNA polymerase II 15 kDa subunit. Relative values are shown in percentages. Error bars represent SD of two independent experiments.

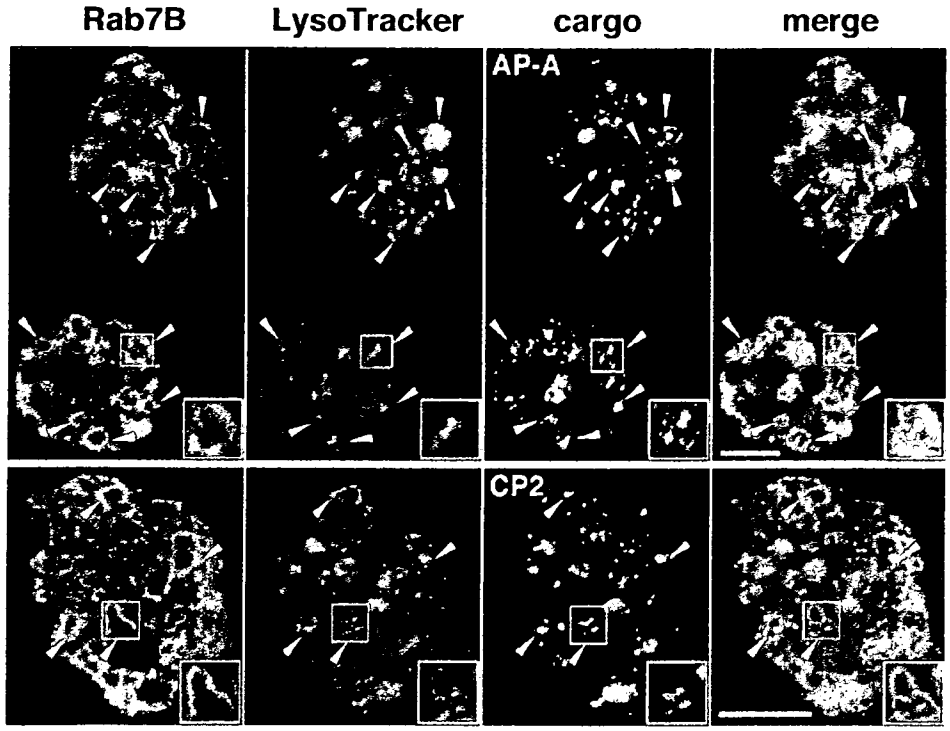

Fig. 2. Immunofluorescence analysis of *Eh*Rab7B. The HA-tagged *Eh*Rab7B-overexpressing transformant was incubated with LysoTracker Red, and subjected to immunofluorescence assay using anti-HA antibody and either anti-AP-A (upper panels) or anti-CP2 antibody (lower panels). Arrowheads indicate representative *Eh*Rab7B-positive vacuoles containing both LysoTracker and AP-A (upper) or both LysoTracker and CP2 (lower). Insets show magnified images of selected *Eh*Rab7B-positive vacuoles. Bars, 10 μm.

Eh*Rab7B is associated with late endosomes/lysosomes and is likely involved in lysosomal maturation*

We examined subcellular localization of *Eh*Rab7B by immunofluorescence assay using a stable transformant that constitutively expressed three tandem haemagglutinin (3HA)-tagged *Eh*Rab7B (Fig. 2). In the transformant, *Eh*Rab7B was found to be associated with 1–4 μm vesicles/vacuoles. Almost all (93% ± 0.7%) *Eh*Rab7B-positive vesicles/vacuoles contained degradative proteins represented by AP-A and CP2, as well as LysoTracker Red, a membrane diffusible probe accumulated in acidic compartments (Bucci *et al.*, 2000). Contrarily, less than 50% of *Eh*Rab7A-positive vacuoles, when overexpressed, contained LysoTracker Red (Nakada-Tsukui *et al.*, 2005), suggesting that *Eh*Rab7B is probably located downstream of *Eh*Rab7A in the maturation of the post-Golgi compartment to lysosomes. The *Eh*Rab7B-associated vacuoles typically contained multi-vesicular structures that included the lysosome-resident proteins and the marker (Fig. 2, insets), which is similar to the structures previously demonstrated in the *Eh*Rab7A vacuoles containing endosomes enclosing the fluid-phase marker (Saito-Nakano *et al.*, 2004).

We also examined the localization of *Eh*Rab7B using the wild-type trophozoites and the anti-*Eh*Rab7B antibody affinity purified by the antigen-immobilized column. Immunoblot assay using anti-*Eh*Rab7B antibody showed a single 23 kDa band in the lysate of the wild-type trophozoites, and 23 and 27 kDa bands in the lysate of the *Eh*Rab7B-overexpressing transformant. The 27 kDa band was also detected with anti-HA antibody, suggesting that the 27 kDa band corresponds to the exogenous epitope-tagged *Eh*Rab7B (Fig. 3A). We roughly estimated by measuring signal of the bands by chemiluminescence assay that the amount of the epitope-tagged *Eh*Rab7B was eightfold higher than that of the endogenous protein (Fig. 3A). Immunofluorescence imaging with the affinity-purified anti-*Eh*Rab7B IgG revealed that intrinsic *Eh*Rab7B was associated with the periphery of lysosomes in wild-type cells (Fig. 3B). The localization of the intrinsic *Eh*Rab7B was similar to, but slightly different from that of the tagged-*Eh*Rab7B in the transformant. In the wild-type cell, enlarged lysosomes, often observed in the tagged-*Eh*Rab7B-expressing transformant (Fig. 2), were occasionally detected. Endogenous *Eh*Rab7B-associated vesicles/vacuoles were often (93.5% ± 7.6%) associated with LysoTracker (Fig. 3B). We also verified that the apparent localization of *Eh*Rab7B in the epitope-tagged *Eh*Rab7B-expressing transformant demonstrated with anti-*Eh*Rab7B antibody was indistinguishable from that using anti-HA antibody

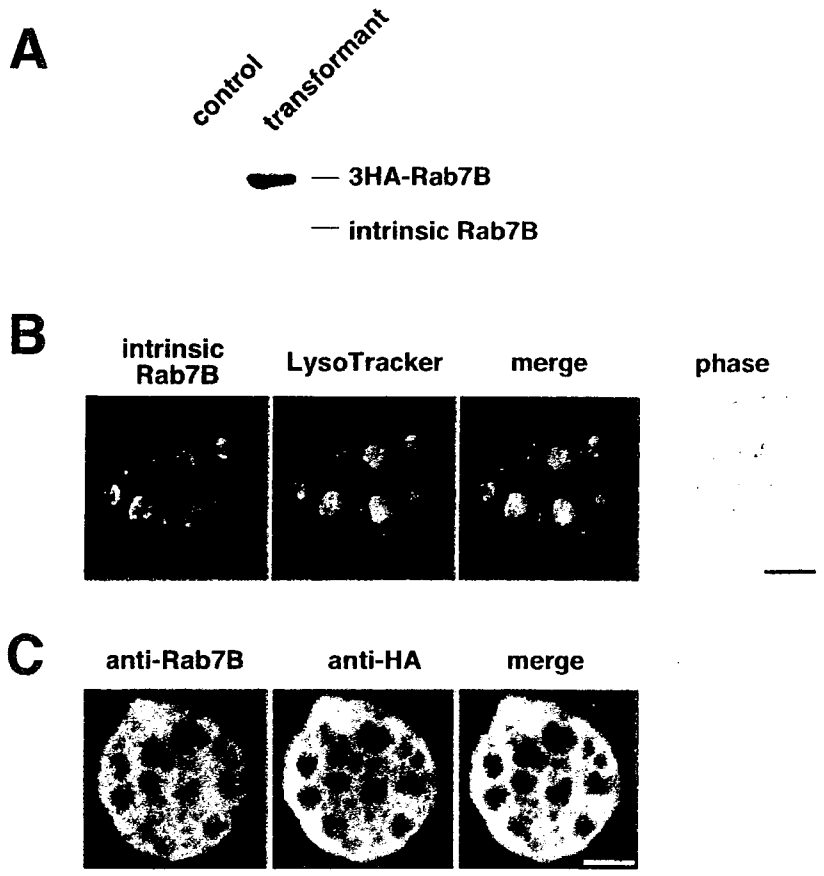

Fig. 3. Detection of intrinsic and epitope-tagged *Eh*Rab7B in wild-type and transformant trophozoites.
A. Immunoblot analysis of intrinsic and exogenous *Eh*Rab7B in wild-type cells (left) and the HA-tagged *Eh*Rab7B-overexpressing transformant (right) using affinity-purified anti-*Eh*Rab7B antibody.
B. Immunofluorescence imaging of intrinsic *Eh*Rab7B in wild-type cells. Lysosomes were stained with LysoTracker Red (red) and intrinsic *Eh*Rab7B was visualized with anti-*Eh*Rab7B antibody (green).
C. Detection of *Eh*Rab7B with anti-*Eh*Rab7B (green) and anti-HA (red) antibodies in the HA-tagged *Eh*Rab7B-overexpressing transformant. Bars, 10 μm.

(Fig. 3C). Taken together, these data suggest that *Eh*Rab7B is primarily associated with late endosomes/lysosomes, and involved in the maturation of the acidic compartment, and that overexpression of *Eh*Rab7B caused enhancement of late endosome/lysosomal fusion and enlargement of lysosomes.

To investigate a role of *Eh*Rab7B in lysosome maturation, the total cellular acidity of the *Eh*Rab7B-overexpressing and control transformants was measured by fluorescence-activated cell sorter (FACS) analysis of the LysoTracker-stained cells (Fig. 4). The LysoTracker staining significantly increased by *Eh*Rab7B overexpression; the peak channel increased from 29 ± 4.5 in the control transformant to 43 ± 2.1 in the *Eh*Rab7B-overexpressing transformant (Fig. 4, left; $P = 0.038$ by Student's *t*-test), indicating that *Eh*Rab7B overexpression increased the volume of the acidic compartment, which is likely attributable to enhanced homotypic or heterotypic lysosome fusion. Similarly, overexpression of *Eh*Rab7A resulted in an augmented formation of *Eh*Rab7A-positive vesicles/vacuoles and an increased cellular acidity (Nakada-Tsukui *et al.*, 2005). Expression of a GTP-form (H69L), corresponding to human Rab7-GTP mutation, of *Eh*Rab7B (*Eh*Rab7B-GTP) slightly reduced the total cel-

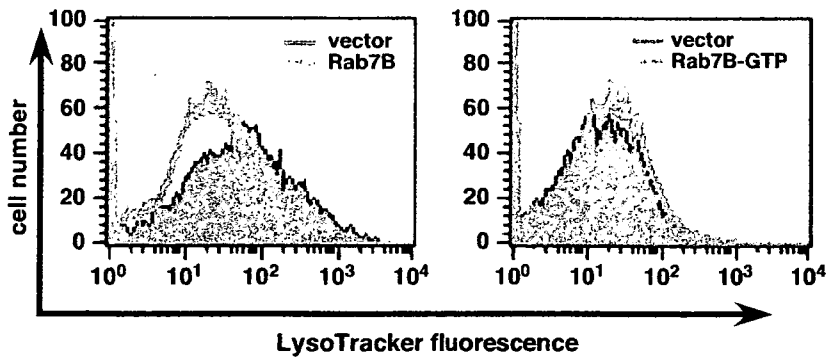

Fig. 4. Histograms of LysoTracker-stained trophozoites of *Eh*Rab7B- (left panel, purple), *Eh*Rab7B-GTP-overexpressing (right panel, purple), and control (vector) (both panels, green) transformants by FACS analysis. The transformants were stained with 2 μM LysoTracker Green for 30 min and then analysed on FACS.

lular acidity (peak channel, 24 ± 3.5; $P = 0.04$ versus the control transformant, Fig. 4, right), which is likely a dominant-negative effect. In contrast, expression of *Eh*Rab7A-GTP further increased the cellular acidity (data not shown), similar to human Rab7-GTP mutant (Bucci *et al.*, 2000).

Eh*Rab7B-GTP form mutant is partially defective in membrane association*

Function of Rab proteins is modulated by hydrolysis and exchange of bound guanine nucleotides (i.e. GTP-bound active and GDP-bound inactive states) (Novick and Zerial, 1997). A majority of GTP-bound Rab proteins are associated with the membrane, and potentially capable of interacting with effectors, while GDP-bound Rab proteins are complexed with GDP-dissociation inhibitor and localized in the cytosol. To better understand the cause of the acidification defect caused by *Eh*Rab7B-GTP, we fractionated the total lysate prepared by mechanical homogenization. Immunoblot analysis revealed that only a half (58% ± 5.6%) of *Eh*Rab7B-GTP was recovered in the 100 000 *g* pellet (membrane) fraction, while a majority (86% ± 3.5%) of wild-type *Eh*Rab7B was detected in this fraction (Fig. 5). These results indicate that membrane association of *Eh*Rab7B-GTP form is partially hampered.

Immunofluorescence imaging of the *Eh*Rab7B-GTP-expressing transformant (Fig. 6A) showed that *Eh*Rab7B-GTP was localized in the cytosol or tiny vesicles throughout the cell in steady state. The *Eh*Rab7B-GTP colocalization with the compartment associated with the lysosomal proteins and marker (AP-A, CP2, and LysoTracker) was less pronounced (Fig. 6B) than that for the wild-type *Eh*Rab7B (Fig. 2). These results were consistent with the defect of membrane association of *Eh*Rab7B-GTP (Fig. 5).

Expression of Eh*Rab7B-GTP form mutant causes missorting of lysosomal proteins*

To reveal the precise role of *Eh*Rab7B in lysosome biogenesis, we next examined if transport of lysosomal cargo proteins, i.e. AP-A and CP2, is affected by overexpression of *Eh*Rab7B wild type or GTP-form mutant. AP-A and CP2 were very well colocalized with LysoTracker in the *Eh*Rab7B-overexpressing transformant (see above, Fig. 2A). In the *Eh*Rab7B-GTP transformant, the colocalization of the lysosomal cargo proteins and LysoTracker remarkably decreased (Fig. 6B; $P = 0.013$ or 0.007 for CP2 or AP-A respectively), suggesting that *Eh*Rab7B-GTP expression caused either hindrance of transport or mistargeting of the lysosomal proteins.

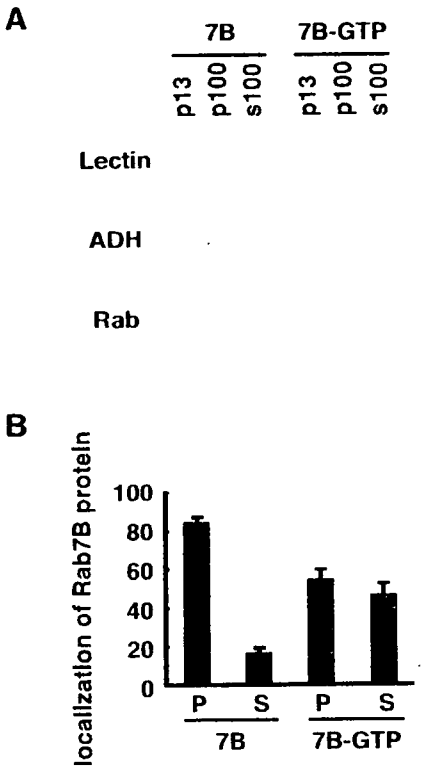

Fig. 5. Subcellular fractionation of *Eh*Rab7B and *Eh*Rab7B-GTP.
A. Fractionation of the lysates from the *Eh*Rab7B and *Eh*Rab7B-GTP transformants. Amoebic total homogenate was separated into low-speed pellet (p13), high-speed pellet (p100) and supernatant (s100) fractions, and these fractions were subjected to immunoblot analyses using the following antibodies: anti-HA antibody to probe *Eh*Rab7B and *Eh*Rab7B-GTP (Rab), anti-Gal/GalNAc-inhibitable lectin antibody (Lectin), anti-alcohol dehydrogenase (ADH) antibody, the latter two of which were used as a marker for the membrane or cytosolic protein respectively.
B. Quantification of *Eh*Rab7B and *Eh*Rab7B-GTP in the fractions separated by differential centrifugation as in (A) by chemiluminescence measurement with LAS3000 Lumi-Imager.

We next measured both secreted and intracellular CP activities of the *Eh*Rab7B-, *Eh*Rab7B-GTP-overexpressing, and control transformants. The CP activity secreted to the medium by the *Eh*Rab7B-GTP transformant was 4.3-fold higher than the control transformant (Fig. 6C, right) ($P = 0.0016$). Moreover, the *Eh*Rab7B-GTP transformant had a 38% less total intracellular CP activity than the control transformant ($P = 0.012$) (Fig. 6C, left). In contrast, neither secreted nor intracellular CP activity significantly changed in the *Eh*Rab7B-overexpressing transformant. To ensure CP production *per se* was not affected by *Eh*Rab7B-GTP overexpression, the steady-state amount of the three major CP (CP1, CP2 and CP5) mRNA was measured by quantitative RT-PCR. The steady-state level of CP1, CP2 or CP5 mRNA remained unchanged in the *Eh*Rab7B-GTP transformant compared with the control transformant

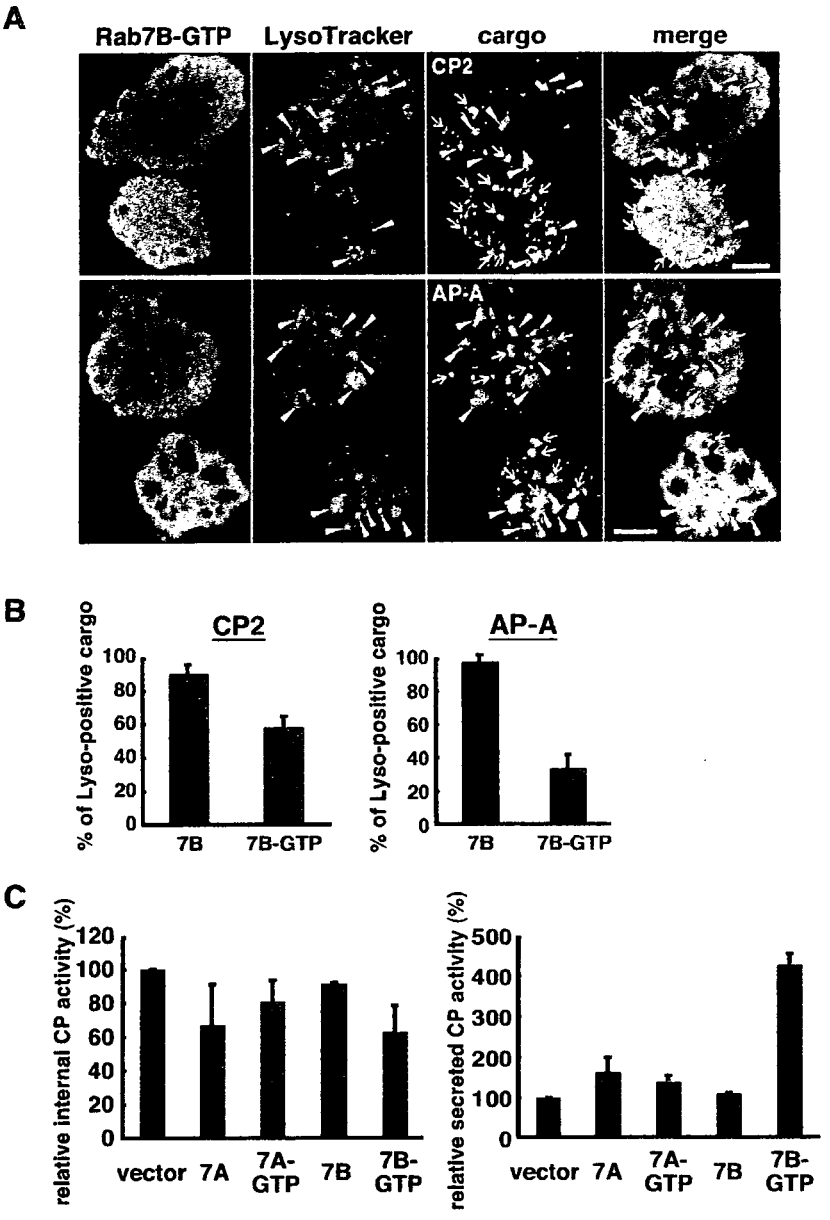

Fig. 6. Localization of *Eh*Rab7B-GTP and effects of *Eh*Rab7B overexpression on CP transport to lysosomes and CP activity.
A. Immunofluorescence assay of *Eh*Rab7B-GTP. Colocalization of lysosomal cargo proteins (blue), CP2 (upper panels) and AP-A (lower panels), with LysoTracker (red) in the *Eh*Rab7B-GTP (green)-expressing transformant. Arrowheads indicate cargo proteins colocalized with LysoTracker. Arrows indicate cargo proteins not associated with LysoTracker. Bars, 10 μm.
B. Measurement of cargo protein transport to lysosomes in the *Eh*Rab7B and *Eh*Rab7B-GTP transformants. Percentages of LysoTracker-positive vesicles/vacuoles of all cargo-positive vesicles/vacuoles are shown.
C. CP activity in the whole lysate (left) and secreted to the medium (right) in the *Eh*Rab7A ('7A'), *Eh*Rab7A-GTP ('7A-GTP'), *Eh*Rab7B ('7B'), *Eh*Rab7B-GTP ('7B-GTP') and control ('vector') transformants. CP activity is shown in percentage relative to that of the control transformant. Error bars represent SD of two independent experiments.

(113%, 86% or 91% of the mRNA level of the control respectively; data not shown). Together with the fact that *Eh*Rab7B overexpression enhanced maturation and/or fusion of the acidic compartment whereas *Eh*Rab7B-GTP conferred the opposite effect (Fig. 4), these data indicate that *Eh*Rab7B may mediate trafficking of lysosomal proteins to the storage compartment. In contrast, overexpression of either *Eh*Rab7A or *Eh*Rab7A-GTP caused the less magnitude (< twofold) of changes of intracellular and secreted CP activity, which is consistent with the premise that *Eh*Rab7B mediates a transport stage closer to lysosomes than that mediated by *Eh*Rab7A.

Eh*Rab7B and* Eh*Rab7A are localized to distinct but significantly overlapping compartments*

We have previously shown that *Eh*Rab7A is associated with the post-Golgi compartment, but not the acidic compartment in steady state (Saito-Nakano *et al.*, 2004). To clarify the difference of subcellular localization between *Eh*Rab7A and *Eh*Rab7B, localization of *Eh*Rab7A and *Eh*Rab7B was simultaneously visualized using the *Eh*Rab7B-overexpressing transformant (Fig. 7A). In steady state, vacuoles associated with either *Eh*Rab7A or *Eh*Rab7B, or both were observed. Approximately one

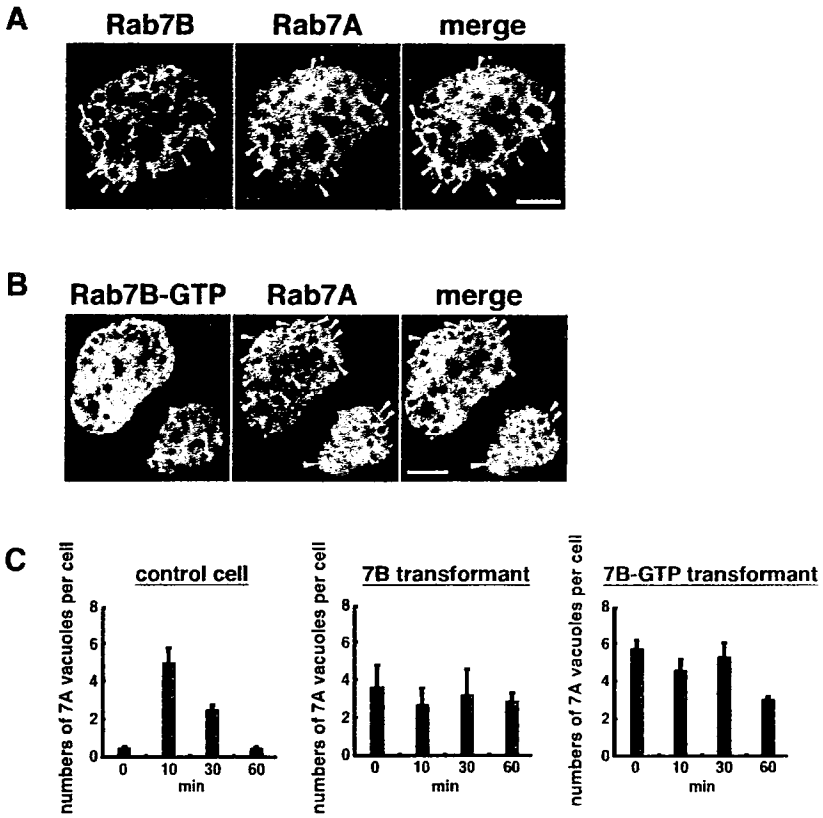

Fig. 7. Subcellular localization of *Eh*Rab7B and *Eh*Rab7A and effects of *Eh*Rab7B overexpression on PPV formation.
A and B. Immunofluorescence images of *Eh*Rab7B, *Eh*Rab7B-GTP and *Eh*Rab7A. The HA-tagged *Eh*Rab7B- (A) or *Eh*Rab7B-GTP (B)-overexpressing transformant was probed with anti-HA (green) and anti-*Eh*Rab7A (red) antibodies to simultaneously visualize *Eh*Rab7B (A) or *Eh*Rab7B-GTP (B) and *Eh*Rab7A respectively. Green or red arrowheads indicate the vacuoles stained solely with either anti-*Eh*Rab7B or *Eh*Rab7A antibody respectively. Vacuoles simultaneously stained with both anti-*Eh*Rab7B and *Eh*Rab7A antibodies are marked with yellow arrowheads. Bars, 10 μm.
C. The number of *Eh*Rab7A-positive vacuoles at 10, 30 and 60 min after phagocytosis of erythrocytes in the control, *Eh*Rab7B- and *Eh*Rab7B-GTP-overexpressing transformants.

fourth (28% ± 4.2%) of *Eh*Rab7B-positive vacuoles were associated with *Eh*Rab7A. Conversely, about a half (60% ± 13%) of *Eh*Rab7A-positive vacuoles were associated with *Eh*Rab7B. The compartment co-associated with both *Eh*Rab7A and *Eh*Rab7B is likely the transitional compartment. The average diameter of *Eh*Rab7A- or *Eh*Rab7B-positive vacuoles was 3.5 ± 0.3 or 3.4 ± 0.1 μm respectively. Localization of *Eh*Rab7A and *Eh*Rab7B was also clearly different during phagocytosis (Fig. 8A). *Eh*Rab7B was not associated with erythrocyte-containing phagosomes whereas *Eh*Rab7A was often localized to them (Saito-Nakano *et al.*, 2004). In addition, *Eh*Rab7B was not associated with one of the retromer-like complex, Vps26, which was shown to be colocalized with *Eh*Rab7A (Nakada-Tsukui *et al.*, 2005) (Fig. 8B).

Eh*Rab7B plays a role in the formation of PPV, phagosomal acidification, and degradation of its content*

We previously reported that PPV is the *Eh*Rab7A-associated preparatory vacuole, formed in response to phagocytosis stimuli, and is necessary for efficient phagocytosis (Saito-Nakano *et al.*, 2004). *Eh*Rab7A-positive PPVs were not present before the addition of erythrocytes, emerged at 10 min after phagocytosis, and disappeared at 30–60 min in the control transformant ('control cell') (Fig. 7C, left). On the other hand, in the *Eh*Rab7B or *Eh*Rab7B-GTP transformants, an average number of 3.3 ± 1.5 or 5.6 ± 2.3 *Eh*Rab7A-positive PPVs per trophozoite were formed in steady state respectively (Fig. 7A–C). This result indicates that overexpression of *Eh*Rab7B or *Eh*Rab7B-GTP induced the formation of PPVs without phagocytosis-linked stimuli (e.g. attachment). Moreover, the number of PPVs in the *Eh*Rab7B- or *Eh*Rab7B-GTP-expressing transformant remained unchanged during erythrophagocytosis (Fig. 7C, middle and right), which was in good contrast to the time-dependent emergence and disappearance of PPV in the course of phagocytosis (Saito-Nakano *et al.*, 2004; Fig. 7C, left). Next, we tested if the *Eh*Rab7B- and *Eh*Rab7B-GTP-expressing transformants, both of which showed defect in the erythrocyte-induced formation of PPVs, are defective in engulfment *per se*. Overexpression of *Eh*Rab7B-GTP or *Eh*Rab7B wild-type, to a less degree, resulted in the reduction of yeast phagocytosis (Fig. 9A). These data agreed with the premise that the interference of the regulation of the PPV formation hindered engulfment, which is similar to the case seen for *Eh*Rab5-GTP (Saito-Nakano *et al.*, 2004).

Acidification and degradation of the content in phagosomes well correlated (Mitra *et al.*, 2005; 2006). We next

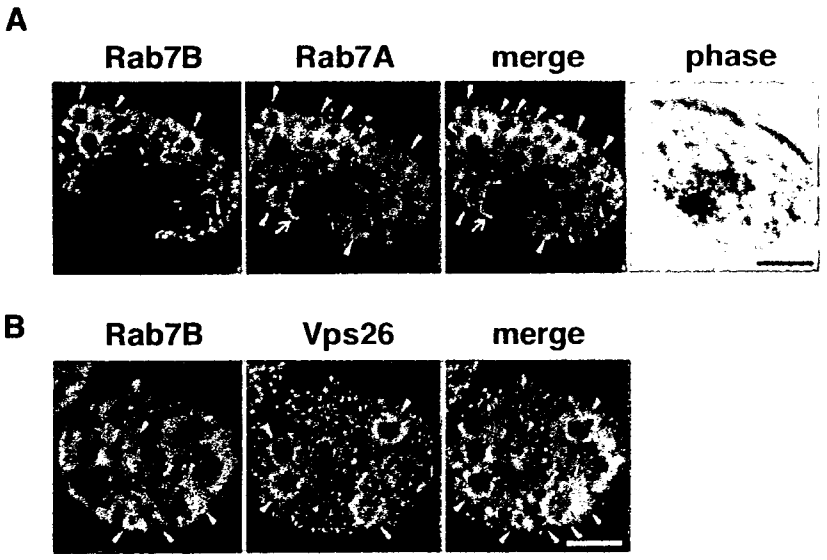

Fig. 8. Immunofluorescence imaging of *Eh*Rab7A, *Eh*Rab7B and retromer-like complex during erythrophagocytosis.
A. Localization of *Eh*Rab7A and *Eh*Rab7B during erythrophagocytosis. The transformant was cultivated with erythrocytes for 30 min and *Eh*Rab7A (red) or HA-tagged *Eh*Rab7B (green) was detected with anti-*Eh*Rab7A or anti-HA antibody respectively. *Eh*Rab7A-single positive, *Eh*Rab7B-single positive, or double-positive vacuoles were shown in red, green or yellow arrowheads respectively. Note that a phagosome containing an erythrocyte (an red arrow, stained black with diaminobenzidine) is associated with *Eh*Rab7A, but not *Eh*Rab7B.
B. Lack of colocalilzation of *Eh*Rab7B and Vps26, one of the components of the retromer-like complex, which was previously shown to be the *Eh*Rab7A effector. Note that *Eh*Rab7B (green) did not colocalize with Vps26 (red), in contrast to colocalization of Vps26 and *Eh*Rab7A (Nakada-Tsukui *et al.*, 2005). Bars, 10 μm.

examined if expression of *Eh*Rab7B or *Eh*Rab7B-GTP affects phagosomal acidification and degradation of ingested materials (Fig. 9B and C). Phagosomes of the *Eh*Rab7B-GTP transformant were less acidic (the average pH of phagosomes of 2–10 min post ingestion, 5.01 ± 0.10) than that of the mock vector control transformant (4.58 ± 0.11, $P = 0.00028$) (Fig. 9B). Moreover, *Eh*Rab7B-GTP transformant showed approximately 25% reduced degradation as measured with decay of GFP fluorescence of ingested GFP-expressing *Leishmania* promastigotes (1.80% ± 0.32% GFP degradation per min), when compared with the vector control transformant (2.40% ± 0.25% degradation per min; $P = 0.025$) (Fig. 9C). These results are consistent with the premise that *Eh*Rab7B-GTP overexpression caused defect in lysosomal acidification and transport of lysosomal proteins (Figs 4 and 6). In contrast, *Eh*Rab7B overexpression, which resulted in enhancement of lysosomal fusion and increase of the lysosome volume, caused no significant change in phagosome pH and degradation kinetics. The average phagosome pH of 2–10 min post ingestion was 4.72 ± 0.12 in the *Eh*Rab7B-overexpressing transformant ($P > 0.05$ versus the control transformant). Degradation within phagosomes in the *Eh*Rab7B transformant (2.00 ± 0.37% degradation per min) was only slightly reduced compared with the mock vector control ($P > 0.05$ versus the control transformant).

Discussion

In the present study, we described the functional differences of Rab7 isotypes in this medically important protozoan parasite. As far as we are concerned, this is the first report on the functional differences between Rab7 isotypes in not only protists, but also unicellular eukaryotes. Rab7 GTPase has been implicated in trafficking of at least three steps in different organisms, i.e. early endosomes to late endosomes in BHK cell (Feng *et al.*, 1995; Vitelli *et al.*, 1997), late endosomes to lysosomes in HeLa cell (Meresse *et al.*, 1995; Bucci *et al.*, 2000), and homotypic lysosome fusion in *S. cerevisiae* (Wichmann *et al.*, 1992; Schimmoller and Riezman, 1993; Haas *et al.*, 1995). Our data presented here are consistent with the notion that *Eh*Rab7B is localized to late endosomes/lysosome and involved in the formation of or fusion to lysosomes, whereas *Eh*Rab7A is associated with the post-Golgi compartment containing cargos destined to lysosomes, and involved in the fusion to late endosomes. There was no precedent where two Rab7 isotypes are involved in the trafficking of lysosomal proteins from the post-Golgi to lysosomes/phagosomes in a sequential and co-ordinated fashion, as shown in this study.

We have demonstrated that the two representative Rab7 isotypes, *Eh*Rab7A and *Eh*Rab7B, showed differences in localization and role in biogenesis of lysosomes

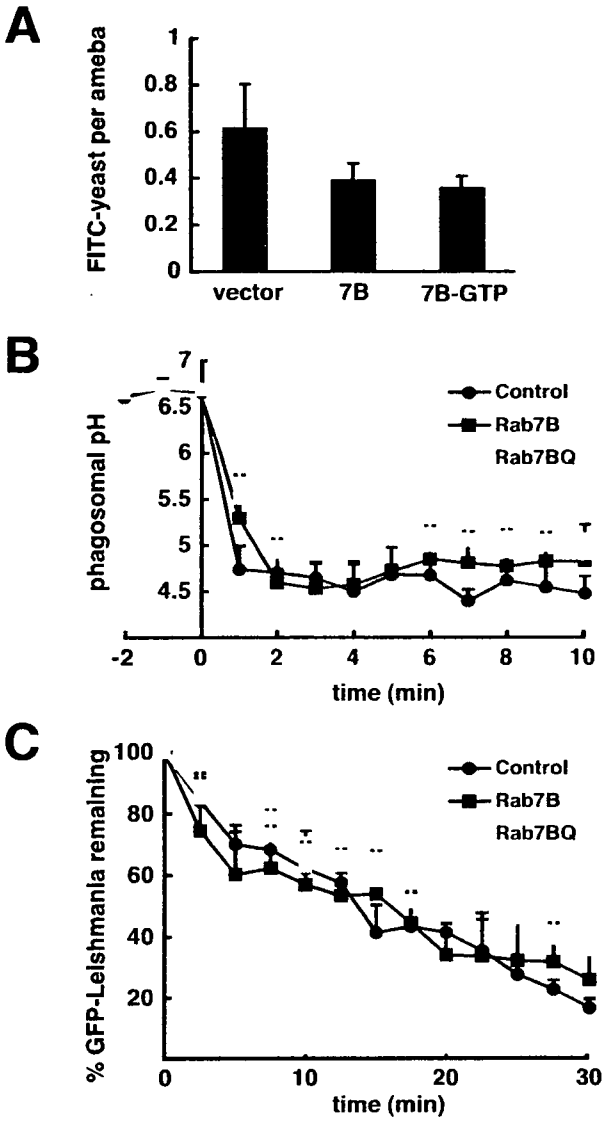

Fig. 9. Effects of *Eh*Rab7B and *Eh*Rab7B-GTP overexpression on phagocytosis efficiency, and acidification and degradation in phagosomes.
A. Phagocytosis of FITC-labelled yeasts by the *Eh*Rab7B-, *Eh*Rab7B-GTP-expressing and control transformants. Trophozoites were incubated with FITC-conjugated yeasts at 1:20 ratio at 33°C for 30 min and ingested yeasts were counted. The average of three independent experiments is shown. Error bars represent SD of the measurement of 300–350 amoebae.
B. Kinetics of phagosome acidification in the *Eh*Rab7B-expressing (black squares), *Eh*Rab7B-GTP-expressing (grey squares) and control (black circles) transformants. Trophozoites were mixed with FITC-labelled yeasts at 1:10 ratio on a glass bottom culture dish, enclosed with a coverslip, and allowed to ingest yeasts at 33°C. Trophozoites containing a single yeast were selected and phagosome pH was measured at 1 min intervals for 3 h with time-lapse video microscopy on a Leica AS MDW. Only data for the first 10 min are shown. Data represent the average of 10 independent phagosomes.
C. Kinetics of degradation of GFP-expressing *Leishmania* promastigotes in the *Eh*Rab7B-expressing (black squares), *Eh*Rab7B-GTP-expressing (grey squares) and control (black circles) transformants. Trophozoites were incubated with live GFP-*Leishmania* promastigotes at 1:5 ratio and images were captured at 30 s intervals to measure the GFP fluorescence intensity. Data of the average of 10 independent phagosomes at 2.5 min intervals are shown.

and phagosomes. First, as mentioned above, while *Eh*Rab7A is primarily localized in the post-Golgi compartment (Saito-Nakano *et al.*, 2004; Nakada-Tsukui *et al.*, 2005), *Eh*Rab7B is almost exclusively localized to late endosomes/lysosomes (Fig. 2). Second, while *Eh*Rab7A is transported to phagosomes containing erythrocytes after 30 min of phagocytosis (Saito-Nakano *et al.*, 2004), *Eh*Rab7B is not trafficked via or to erythrocyte-containing phagosomes (Fig. 8A). Third, overexpression of *Eh*Rab7B-GTP dramatically decreased intracellular CP activity and enhanced secretion of CP activity into the medium, while overexpression of *Eh*Rab7A or *Eh*Rab7A-GTP affected intracellular and secreted CP activity only marginally (Fig. 6C). Fourth, *Eh*Rab7A regulates retrograde transport of a putative hydrolase receptor from phagosomes to the *trans*-Golgi network via interaction with the retromer-like complex (Nakada-Tsukui *et al.*, 2005), while *Eh*Rab7B neither interacts with the retromer-like complex nor is associated with the process (Fig. 8B). On the other hand, overexpression of these two Rab7 isotypes led to apparently similar consequences. Overexpression of *Eh*Rab7A or *Eh*Rab7B caused increase of the cellular acidity, consistent with the notion that *Eh*Rab7A or *Eh*Rab7B is involved in maturation of and fusion to late endosomes or lysosomes respectively. Neither *Eh*Rab7A nor *Eh*Rab7B overexpression caused defect in endocytosis or growth (data not shown), suggesting lack of association of these Rab7 isotypes with initial phase of endocytosis or recycling.

It is conceivable that *Eh*Rab7A and *Eh*Rab7B share common effectors, and transmit signal for divergent pathways because the effector domain of these two Rab7 isotypes showed 90% identity [YKATIGADF*L*, a.a. 36–45 of *Eh*Rab7A; YKATIGADF*M*, a.a. 39–48 of *Eh*Rab7B; substituted amino acids are shown in italic] (Saito-Nakano *et al.*, 2005). Mechanisms by which activation of *Eh*Rab7A leads to recruitment and activation of *Eh*Rab7B may exist, as shown for the case of endosome maturation in mammalian cells, where Rab5 recruited to early endosomes initiates recruitment of the HOPS complex, an effector complex of Rab7 essential for lysosome fusion (Eitzen *et al.*, 2000), and Rab7-guanine nucleotide exchange factor in the complex further activates Rab7 for following maturation of endosomes (Rink *et al.*, 2005).

The decrease of the cellular acidity caused by *Eh*Rab7B-GTP expression may be at least partially attributable to its disrupted membrane association of this

mutant. In HeLa cell, expression of Rab7-GTP conferred dominant active phenotypes, e.g. augmented lysosomal fusion and formation of enlarged lysosomes (Bucci *et al.*, 2000). The unexpected dominant-negative phenotypes such as reduction of the lysosome acidity, CP and AP-A transport to lysosomes, and phagosome acidification and degradation, observed in the *Eh*Rab7B-GTP mutant, was also observed in the case of *Eh*Rab5-GTP overexpression, which caused a defect in the formation of PPV and phagocytosis efficiency (Saito-Nakano *et al.*, 2004). Alternative explanations for the dominant-negative phenotype include: *Eh*Rab7B-GTP elicited irreversible recruitment of and binding to the HOPS complex, or its amoebic equivalent, which interfered with downstream maturation due to incompetence of GTP hydrolysis (Bowers and Stevens, 2005). Similarly, it was shown that Ypt7-GDP mutant was unable to recruit the HOPS complex in yeast, and incompetent to initiate vacuole docking and fusion (Eitzen *et al.*, 2000).

Mislocalization of lysosomal cargos to non-acidified compartments observed in the *Eh*Rab7B-GTP-expressing transformant (Fig. 6B) is similar to the previous demonstration that expression of a Rab7 mutant inhibited lysosomal acidification, due to perturbation of V-ATPase (Bucci *et al.*, 2000). In yeast, defects in genes involved in transport from the *trans*-Golgi to the vacuole showed missecretion of vacuolar proteases to the medium (Bowers and Stevens, 2005). Although mechanisms of the CP missecretion to the extracellular milieu is not well understood, it is conceivable to hypothesize that mislocalized lysosomal proteins are transported to the plasma membrane through recycling pathway mediated by *Eh*Rab11B, which plays a substantial role in the secretion of CPs (Mitra *et al.*, 2007).

Overexpression of *Eh*Rab7B or *Eh*Rab7B-GTP caused reduction of the phagocytosis efficiency. In addition, attachment-dependent formation and disintegration of PPVs were interrupted by overexpression of either *Eh*Rab7B or *Eh*Rab7B-GTP (Fig. 7C). In wild-type amoebae, PPVs emerged in a contact-dependent manner, and disappeared after 20–30 min after phagocytosis (Saito-Nakano *et al.*, 2004). In contrast, in the *Eh*Rab7B- or *Eh*Rab7B-GTP-overexpressing transformant, PPVs were formed in quiescent state, and the formation and disassembly of PPVs were not controlled in a course of phagocytosis (Fig. 7C). These data are consistent with the notion that *Eh*Rab7B is involved in the signalling associated with phagocytosis. *Eh*Rab7B-GTP expression also caused defect in phagosome acidification, which correlated well with retardation in the degradation of the content within phagosomes (Fig. 9B and C). The negative effects of *Eh*Rab7B-GTP on phagosome functions can be explained as a decreased efficiency of recruitment of V-ATPase and transport of digestive proteins to lysosomes and phagosomes.

Five of Rab7 isotypes (*Eh*Rab7A, B, C, D and E) were identified from the latex bead-containing phagosomes isolated by flotation centrifugation on a sucrose step gradient (Okada *et al.*, 2005; 2006) and three of them (Fig. 7A, B and D) were also identified from phagosomes containing human serum-coated magnetic beads (Marion *et al.*, 2005). These *Eh*Rab7 isotypes revealed remarkable stage-dependent recruitment to phagosomes during maturation. e.g. *Eh*Rab7A and *Eh*Rab7E are constitutively associated with phagosomes while *Eh*Rab7B, *Eh*Rab7C and *Eh*Rab7D were detected in an early (0–30 min) to intermediate phase (60 min). Thus, it is conceivable that that these *Eh*Rab7 isotypes are sequentially and co-ordinately involved in phagosome biogenesis. Other not-yet-characterized phagosome-associated *Eh*Rab7 isotypes, i.e. *Eh*Rab7C, 7D and 7E, likely play an independent role in the lysosome/phagosome trafficking in this organism. Finally, the multiplicity and diversity of *Eh*Rab7 isotypes reflect the complexity and biological importance of endosomal–lysosomal trafficking and phagosome biogenesis in this organism, which may be related to parasitism and virulence of this medically important parasite.

Experimental procedures

Culture

Trophozoites of the *E. histolytica* isolate HM-1:IMSS cl6 (Diamond *et al.*, 1972) were cultured axenically in BI-S-33 medium at 35°C as described previously (Diamond *et al.*, 1978).

Quantitative RT-PCR

mRNA expression of nine *Eh*Rab7 genes (Saito-Nakano *et al.*, 2005) and three major CPs (CP1, CP2 and CP5) was analysed by quantitative RT-PCR analysis essentially as previously described (Gilchrist *et al.*, 2006) with some modifications. RNA polymerase II served as an internal control (GenBank accession number, XP_649091) (Gilchrist *et al.*, 2006). Primers used were 5′-gctgaacaatggtgttcagaacat-3′ and 5′-caaaagtctgattgccc ttgttga-3′ (*Eh*Rab7A, GenBank Accession No. AB054583); 5′-gaccaattaaggcaatggtgtgtt-3′ and 5′-acacaatcatcttgtagctgc taa-3′ (*Eh*Rab7B, AB186363); 5′-gcaaaagattggtgtgaaaataat-3′ and 5′-gaaccaaataagagctgttgttaa-3′ (*Eh*Rab7C, AB186364); 5′-gaacaagcacgagaatggtgtaaa-3′ and 5′-aagaaagaaggagggtgttg ctaa-3′ (*Eh*Rab7D, AB186365); 5′-tctgatgtaaaacaatggtgtgaa-3′ and 5′-aaaaaagaaggagggtgttgttga-3′ (*Eh*Rab7E, AB186366); 5′-gctgttgatgattggattcaattt-3′ and 5′-gttgaacaagcgccttgttgttaa-3′ (*Eh*Rab7F, AB186367); 5′-gtttcaactgaaagtgctcgtcaa-3′ and 5′-tta acaacaaccactttcagactt-3′ (*Eh*Rab7G, AB186368); 5′-gttgataaaag tcaagaaagagta-3′ and 5′-tcaacaacattgtttttgtgaac-3′ (*Eh*Rab7H, AB186369); 5′-gatgaagaaagacaagttagtttt-3′ and 5′-tcaacaacaa tctttttaaccttt-3′ (*Eh*Rab7I, AB197056); 5′-caatgcaagaataactat tttgca-3′ and 5′-tcagagatattcaacaccagttgg-3′ (CP1, XM_645064);

5′-aaatgcaagaataactactttgct-3′ and 5′-tcaaagatattgaacgccagtt gg-3′ (CP2, XM_645550); 5′-aaagaatgttcatcaactcagctt-3′ and 5′-ttaagcatcagcaaccccaactgg-3′ (CP5, XM_645845); and 5′-gatc caacatatcctaaaacaaca-3′ and 5′-tcaattattttctgacccgtcttc-3′ (RNA polymerase II). Parameters used are: an initial step of denaturation at 95°C for 9 min, followed by 40 cycles of denaturation at 94°C for 30 s, annealing at 50°C for 30 s, and extension at 65°C for 1 min. A final step at 95°C for 9 s, 60°C for 9 s, and 95°C for 9 s was used to remove primer dimers.

Plasmid constructs

A 624 bp DNA fragment containing *EhRab7B* coding sequence was amplified by PCR from *E. histolytica* cDNA library (Nozaki *et al.*, 1998) using a pair of appropriate primers with restriction enzyme sites. The amplified fragment was cloned into the BglII-XhoI sites of pEhEx (Nozaki *et al.*, 1999), and 3HA-tag was inserted at the amino terminus of *Eh*Rab7B gene essentially as described previously (Saito-Nakano *et al.*, 2004). The final plasmid to express 3HA-*Eh*Rab7B in trophozoites was designated pH7B. A plasmid to express *Eh*Rab7B H69L mutant was constructed by PCR-mediated mutagenesis (Landt *et al.*, 1990) and designated pH7BL. A coding region of monomeric red fluorescence protein (mRFP1) was amplified by PCR using mRFP1-pRSETB plasmid (a kind gift from Atsushi Miyawaki) (De Ray *et al.*, 2004) as a template, and cloned into pKT-3M (Saito-Nakano *et al.*, 2004), which contained the cysteine synthase promoter, 3myc-tag, SmaI and XhoI restriction sites to produce pKT-MR. A coding sequence lacking the stop codon of *Eh*Rab7B wild type or H69L mutant was ligated into SmaI-XhoI sites of pKT-MR in frame to the coding region of mRFP1 at the amino terminus to produce pKT-RFP7B and pKT-RFP7BL respectively. The plasmids were introduced into trophozoites by liposome-mediated transfection as previously described (Nozaki *et al.*, 1999; Saito-Nakano *et al.*, 2004), and stable transformants were cultured in the medium containing 6 (for pH7B, pH7BL and pEhEx) or 40 μg ml^{-1} Geneticin (Life Tech Oriental) (for pKT-RFP7B, pKT-RFP7BL and pKT-MR).

Production of antibody

Antiserum was raised against recombinant *Eh*Rab7B in rabbits commercially (Kitayama-Rabes, Japan). IgG was further purified using HiTrap NHS-activated HP column (Amersham) coupled with purified recombinant *Eh*Rab7B according to the manufacture's instruction.

Indirect immunofluorescence

Indirect immunofluorescence assay was conducted as previously described (Saito-Nakano *et al.*, 2004). Trophozoites were transferred to 8 mm round wells on a slide glass, fixed, permeabilized, and reacted with anti-HA 16B12 monoclonal antibody to detect HA-tagged *Eh*Rab7B wild type and *Eh*Rab7B-GTP mutant (Berkeley Antibody), anti-CP2 (a gift from Iris Bruchhaus and Egbert Tannich) (Hellberg *et al.*, 2000), anti-AP-A (a gift from Matthias Leippe) (Leippe *et al.*, 1991), or anti-*Eh*Rab7A, anti-*Eh*Rab7B antibody (Saito-Nakano *et al.*, 2004). Acidic compartments of trophozoites were stained with LysoTracker Red DND-99 (Invitrogen) at 35°C for 12 h.

Flow cytometry

Trophozoites were incubated in BI-S-33 medium containing 2 μM LysoTracker Green (Invitrogen) at 36°C for 30 min, washed with cold phosphate-buffered saline (PBS), and analysed by FACS using FACS Calibur (Becton Dickinson, San Jose, CA) as previously described (Nakada-Tsukui *et al.*, 2005).

Subcellular fractionation

Approximately 3 × 10^5 amoeba cells were washed with cold PBS containing 2% glucose, resuspended in homogenization buffer (250 mM sucrose, 50 mM Tris, pH 7.5, 50 mM NaCl, 0.1 mg ml^{-1} E-64), and homogenized on ice with 30 strokes by a Dounce homogenizer with a tight fitting pestle as described (Okada *et al.*, 2005). After unbroken cells were removed by centrifugation at 4500 *g* for 2 min, the supernatant was centrifuged at 13 000 *g* at 4°C for 10 min to obtain the pellet (p13) and supernatant (s13) fractions. The s13 fraction was further separated by centrifugation at 100 000 *g* at 4°C for 1 h to obtain the pellet (p100) and soluble (s100) fractions. These fractions were subjected to immunoblot analyses with anti-HA, anti-intermediate subunit of Gal/GalNAc-inhibitable lectin (a gift from Hiroshi Tachibana) (Cheng *et al.*, 1998), or anti-alcohol dehydrogenase antibody (Sanuki *et al.*, 2001).

CP assay

Approximately 4 × 10^5 trophozoites were incubated in 100 ml of Opti-MEM medium (Invitrogen), supplemented with 137 mM cysteine and 19 mM ascorbic acid, pH 6.8, on a 96 well micro plate at 35°C for 1 h. After incubation, the culture supernatant was recovered and trophozoites were removed from the micro plate by incubation on ice. CP activity was measured using z-Arg-Arg-7-amino-4-trifluoromethylcoumarin substrate as described (Nakada-Tsukui *et al.*, 2005).

Measurement of phagocytosis efficiency, and acidification and degradation within phagosomes

Phagocytosis of yeasts was monitored as described (Mitra *et al.*, 2005; 2006) with some modifications. Trophozoites transfected with pKT-MR, pKT-RFP7B or pKT-RFP7BL were first monitored for mRFP1 fluorescence to select cells that expressed a high level of mRFP1-*Eh*Rab7B wild type or GTP mutant. Kinetics of acidification of phagosomes and degradation of their contents was monitored using fluorescein isothiocyanate (FITC)-labelled yeasts and GFP-expressing *Leishmania amazonensis* promastigotes respectively, using pKT-MR, pKT-RFP7B or pKT-RFP7BL expressing cells as described previously (Mitra *et al.*, 2005; 2006).

Acknowledgements

The authors thank Shin-ichiro Kawazu and K.P. Chang for the GFP-expressing *Leishmania* strain, Iris Bruchhaus and Egbert Tannich for CP2 antibody, Matthias Leippe for AP-A antibody, and Hiroshi Tachibana for anti-Gal/GalNAc-inhibitable lectin intermediate subunit monoclonal antibody, Atsushi Miyawaki for mRFP1-

expressing plasmid. We thank Yasuo Shigeta and Mai Nudejima for technical assistance. This work was supported by Grant-in-Aid for Scientific Research from the Ministry of Education, Culture, Sports, Science and Technology of Japan to Y.S-N. (17790282) and T.N. (17390124, 18050006, 18073001), a grant for the Research on Health Sciences Focusing on Drug Innovation from Japan Health Sciences Foundation to Y.S.-N. (KH23331) and T.N. (KA11501).

References

Ackers, J.P., Dhir, V., and Field, M.C. (2005) A bioinformatic analysis of the *RAB* genes of *Trypanosoma brucei*. *Mol Biochem Parasitol* **141:** 89–97.

Berriman, M., Ghedin, E., Hertz-Fowler, C., Blandin, G., Renauld, H., Bartholomeu, D.C., *et al.* (2005) The genome of the African trypanosome *Trypanosoma brucei*. *Science* **309:** 416–422.

Borg, S., Brandstrup, B., Jensen, T.J., and Poulsen, C. (1997) Identification of new protein species among 33 different small GTP-binding proteins encoded by cDNAs from *Lotus japonicus*, and expression of corresponding mRNAs in developing root nodules. *Plant J* **11:** 237–250.

Bowers, K., and Stevens, T.H. (2005) Protein transport from the late Golgi to the vacuole in the yeast *Saccharomyces cerevisiae*. *Biochim Biophys Acta* **1744:** 438–454.

Bruchhaus, I., Roeder, T., Lotter, H., Schwerdtfeger, M., and Tannich, E. (2002) Differential gene expression in *Entamoeba histolytica* isolated from amoebic liver abscess. *Mol Microbiol* **44:** 1063–1072.

Bucci, C., Thomsen, P., Nicoziani, P., McCarthy, J., and van Deurs, B. (2000) Rab7: a key to lysosome biogenesis. *Mol Biol Cell* **11:** 467–480.

Cheng, X.J., Tsukamoto, H., Kaneda, Y., and Tachibana, H. (1998) Identification of the 150-kDa surface antigen of *Entamoeba histolytica* as a galactose- and N-acetyl-D-galactosamine-inhibitable lectin. *Parasitol Res* **84:** 632–639.

De Ray, P.A., Min, J.J., Tsien, R.Y., and Gambhir, S.S. (2004) Imaging tri-fusion multimodality reporter gene expression in living subjects. *Cancer Res* **64:** 1323–1330.

Diamond, L.S., Mattern, C.F., and Bartgis, I.L. (1972) Viruses of *Entamoeba histolytica*. I. Identification of transmissible virus-like agents. *J Virol* **9:** 326–341.

Diamond, L.S., Harlow, D.R., and Cunnick, C.C. (1978) A new medium for the axenic cultivation of *Entamoeba histolytica* and other *Entamoeba*. *Trans R Soc Trop Med Hyg* **72:** 431–432.

Eitzen, G., Will, E., Gallwitz, D., Haas, A., and Wickner, W. (2000) Sequential action of two GTPases to promote vacuole docking and fusion. *EMBO J* **19:** 6713–6720.

Feng, Y., Press, B., and Wandinger-Ness, A. (1995) Rab 7: an important regulator of late endocytic membrane traffic. *J Cell Biol* **131:** 1435–1452.

Gilchrist, C.A., Houpt, E., Trapaidze, N., Fei, Z., Crasta, O., Asgharpour, A., *et al.* (2006) Impact of intestinal colonization and invasion on the *Entamoeba histolytica* transcriptome. *Mol Biochem Parasitol* **147:** 163–176.

Haas, A., Scheglmann, D., Lazar, T., Gallwitz, D., and Wickner, W. (1995) The GTPase Ypt7p of *Saccharomyces cerevisiae* is required on both partner vacuoles for the homotypic fusion step of vacuole inheritance. *EMBO J* **14:** 5258–5270.

Haque, R., Huston, C.D., Hughes, M., Houpt, E., and Petri, W.A., Jr. (2003) Amebiasis. *N Engl J Med* **348:** 1565–1573.

Hellberg, A., Leippe, M., and Bruchhaus, I. (2000) Two major 'higher molecular mass proteinases' of *Entamoeba histolytica* are identified as cysteine proteinases 1 and 2. *Mol Biochem Parasitol* **105:** 305–309.

Huston, C.D. (2004) Parasite and host contributions to the pathogenesis of amebic colitis. *Trends Parasitol* **20:** 23–26.

Lal, K., Field, M.C., Carlton, J.M., Warwicker, J., and Hirt, R.P. (2005) Identification of a very large Rab GTPase family in the parasitic protozoan *Trichomonas vaginalis*. *Mol Biochem Parasitol* **143:** 226–235.

Landt, O., Grunert, H.P., and Hahn, U. (1990) A general method for rapid site-directed mutagenesis using the polymerase chain reaction. *Gene* **96:** 125–128.

Leippe, M. (1999) Antimicrobial and cytolytic polypeptides of amoeboid protozoa-effector molecules of primitive phagocytes. *Dev Comp Immunol* **23:** 267–279.

Leippe, M., Ebel, S., Schoenberger, O.L., Horstmann, R.D., and Muller-Eberhard, H.J. (1991) Pore-forming peptide of pathogenic *Entamoeba histolytica*. *Proc Natl Acad Sci USA* **88:** 7659–7663.

Marion, S., Laurent, C., and Guillen, N. (2005) Signalization and cytoskeleton activity through myosin IB during the early steps of phagocytosis in *Entamoeba histolytica*: a proteomic approach. *Cell Microbiol* **7:** 1504–1518.

Mazel, A., Leshem, Y., Tiwari, B.S., and Levine, A. (2004) Induction of salt and osmotic stress tolerance by overexpression of an intracellular vesicle trafficking protein AtRab7 (AtRabG3e). *Plant Physiol* **134:** 118–128.

Meresse, S., Gorvel, J.P., and Chavrier, P. (1995) The rab7 GTPase resides on a vesicular compartment connected to lysosomes. *J Cell Sci* **108:** 3349–3358.

Mitra, B.N., Yasuda, T., Kobayashi, S., Saito-Nakano, Y., and Nozaki, T. (2005) Differences in morphology of phagosomes and kinetics of acidification and degradation in phagosomes between the pathogenic *Entamoeba histolytica* and the non-pathogenic *Entamoeba dispar*. *Cell Motil Cytoskeleton* **62:** 84–99.

Mitra, B.N., Kobayashi, S., Saito-Nakano, Y., and Nozaki, T. (2006) *Entamoeba histolytica*: differences in phagosome acidification and degradation between attenuated and virulent strains. *Exp Parasitol* **114:** 57–61.

Mitra, B.N., Saito-Nakano, Y., Nakada-Tsukui, K., Sato, D., and Nozaki, T. (2007) Rab11B small GTPase regulates secretion of cysteine proteases in the enteric protozoan parasite *Entamoeba histolytica*. *Cell Microbiol* (in press).

Mullins, C., and Bonifacino, J.S. (2001) The molecular machinery for lysosome biogenesis. *Bioessays* **23:** 333–343.

Nakada-Tsukui, K., Saito-Nakano, Y., Ali, V., and Nozaki, T. (2005) A retromerlike complex is a novel Rab7 effector that is involved in the transport of the virulence factor cysteine protease in the enteric protozoan parasite *Entamoeba histolytica*. *Mol Biol Cell* **16:** 5294–5303.

Novick, P., and Zerial, M. (1997) The diversity of Rab proteins in vesicle transport. *Curr Opin Cell Biol* **9:** 496–504.

Nozaki, T., and Nakada-Tsukui, K. (2006) Membrane trafficking as a virulence mechanism of the enteric protozoan

parasite *Entamoeba histolytica*. *Parasitol Res* **98:** 179–183.

Nozaki, T., Asai, T., Kobayashi, S., Ikegami, F., Noji, M., Saito, K., and Takeuchi, T. (1998) Molecular cloning and characterization of the genes encoding two isoforms of cysteine synthase in the enteric protozoan parasite *Entamoeba histolytica*. *Mol Biochem Parasitol* **97:** 33–44.

Nozaki, T., Asai, T., Sanchez, L.B., Kobayashi, S., Nakazawa, M., and Takeuchi, T. (1999) Characterization of the gene encoding serine acetyltransferase, a regulated enzyme of cysteine biosynthesis from the protist parasites *Entamoeba histolytica* and *Entamoeba dispar*. Regulation and possible function of the cysteine biosynthetic pathway in *Entamoeba*. *J Biol Chem* **274:** 32445–32452.

Okada, M., Huston, C.D., Mann, B.J., Petri, W.A., Jr, Kita, K., and Nozaki, T. (2005) Proteomic analysis of phagocytosis in the enteric protozoan parasite *Entamoeba histolytica*. *Eukaryot Cell* **4:** 827–831.

Okada, M., Huston, C.D., Oue, M., Mann, B.J., Petri, W.A., Jr, Kita, K., and Nozaki, T. (2006) Kinetics and strain variation of phagosome proteins of *Entamoeba histolytica* by proteomic analysis. *Mol Biochem Parasitol* **145:** 171–183.

Pereira-Leal, J.B., and Seabra, M.C. (2001) Evolution of the Rab family of small GTP-binding proteins. *J Mol Biol* **313:** 889–901.

Que, X., Brinen, L.S., Perkins, P., Herdman, S., Hirata, K., Torian, B.E., *et al.* (2002) Cysteine proteinases from distinct cellular compartments are recruited to phagocytic vesicles by *Entamoeba histolytica*. *Mol Biochem Parasitol* **119:** 23–32.

Quevillon, E., Spielmann, T., Brahimi, K., Chattopadhyay, D., Yeramian, E., and Langsley, G. (2003) The *Plasmodium falciparum* family of Rab GTPases. *Gene* **306:** 13–25.

Rink, J., Ghigo, E., Kalaidzidis, Y., and Zerial, M. (2005) Rab conversion as a mechanism of progression from early to late endosomes. *Cell* **122:** 735–749.

Saito-Nakano, Y., Yasuda, T., Nakada-Tsukui, K., Leippe, M., and Nozaki, T. (2004) Rab5-associated vacuoles play a unique role in phagocytosis of the enteric protozoan parasite *Entamoeba histolytica*. *J Biol Chem* **279:** 49497–49507.

Saito-Nakano, Y., Loftus, B.J., Hall, N., and Nozaki, T. (2005) The diversity of Rab GTPases in *Entamoeba histolytica*. *Exp Parasitol* **110:** 244–252.

Sanuki, J., Nakano, K., Tokoro, M., Nozaki, T., Okuzawa, E., Kobayashi, S., and Asai, T. (2001) Purification and identification of major soluble 40-kDa antigenic protein from *Entamoeba histolytica*: its application for serodiagnosis of asymptomatic amebiasis. *Parasitol Int* **50:** 73–80.

Schimmoller, F., and Riezman, H. (1993) Involvement of Ypt7p, a small GTPase, in traffic from late endosome to the vacuole in yeast. *J Cell Sci* **106:** 823–830.

Vieira, O.V., Bucci, C., Harrison, R.E., Trimble, W.S., Lanzetti, L., Gruenberg, J., *et al.* (2003) Modulation of Rab5 and Rab7 recruitment to phagosomes by phosphatidylinositol 3-kinase. *Mol Cell Biol* **23:** 2501–2514.

Vines, R.R., Ramakrishnan, G., Rogers, J.B., Lockhart, L.A., Mann, B.J., and Petri, W.A., Jr. (1998) Regulation of adherence and virulence by the *Entamoeba histolytica* lectin cytoplasmic domain, which contains a β2 integrin motif. *Mol Biol Cell* **9:** 2069–2079.

Vitelli, R., Santillo, M., Lattero, D., Chiariello, M., Bifulco, M., Bruni, C.B., and Bucci, C. (1997) Role of the small GTPase Rab7 in the late endocytic pathway. *J Biol Chem* **272:** 4391–4397.

Welter, B.H., Laughlin, R.C., and Temesvari, L.A. (2002) Characterization of a Rab7-like GTPase, EhRab7: a marker for the early stages of endocytosis in *Entamoeba histolytica*. *Mol Biochem Parasitol* **121:** 254–264.

Wichmann, H., Hengst, L., and Gallwitz, D. (1992) Endocytosis in yeast: evidence for the involvement of a small GTP-binding protein (Ypt7p). *Cell* **71:** 1131–1142.

Cellular Microbiology (2007) 9(9), 2112–2125

doi:10.1111/j.1462-5822.2007.00941.x
First published online 17 April 2007

Rab11B small GTPase regulates secretion of cysteine proteases in the enteric protozoan parasite *Entamoeba histolytica*

Biswa Nath Mitra,[1] Yumiko Saito-Nakano,[2] Kumiko Nakada-Tsukui,[1] Dan Sato[1] and Tomoyoshi Nozaki[1]*

[1]*Department of Parasitology, Gunma University Graduate School of Medicine, 3-39-22 Showa-machi, Maebashi, Gunma 371-851, Japan.*

[2]*Department of Parasitology, National Institute of Infectious Diseases, 1-23-1 Toyama, Shinjuku-ku, Tokyo 162-8640, Japan.*

Summary

Vesicular trafficking plays a pivotal role in the virulence of the enteric protozoan parasite *Entamoeba histolytica*. In the present study, we showed that one isotype of the small GTPase Rab11, *Eh*Rab11B, plays a central role in the secretion of a major virulence factor, cysteine proteases. *Eh*Rab11B did not colocalize with markers for the endoplasmic reticulum, early endosomes and lysosomes, but was partially associated with non-acidified vesicles in the endocytic pathway, likely recycling endosomes. Overexpression of *Eh*Rab11B resulted in a remarkable increase in both intracellular and secreted cysteine protease activity, concomitant with an augmentation of cytolytic activity as demonstrated by an increased ability to destroy mammalian cells. The oversecretion of cysteine proteases with *Eh*Rab11B overexpression was neither sensitive to brefeldin A nor specific to a certain cysteine protease species (e.g. CP1, 2 or 5), suggesting that these three major cysteine proteases are trafficked via an *Eh*Rab11B-associated secretory pathway, which is distinct from the classical brefeldin-sensitive pathway. Overexpression of *Eh*Rab11B also enhanced exocytosis of the incorporated fluid-phase marker, supporting the notion that it is involved in recycling. This is the first report demonstrating that Rab11 plays a central role in the transport and secretion of pathogenic factors.

Received 1 November, 2006; revised 7 February, 2007; accepted 23 February, 2007. *For correspondence. E-mail nozaki@med.gunma-u.ac.jp; Tel. (+81) 27 220 8020; Fax (+81) 27 220 8025.

Introduction

Rab proteins are members of the Ras super-family of small GTPases and essential to the regulation of vesicular trafficking in the endocytic and exocytic/secretory pathways in eukaryotic cells (Zerial and McBride, 2001). Rab GTPases are localized to discrete membrane-bound compartments, where they have a specific role depending on the kind and location of Rab (Novick and Zerial, 1997; Chavrier and Goud, 1999). From fission yeast to mammals and higher plants, the Rab family has expanded significantly; the diversity of these proteins is often regarded as a reflection of membrane trafficking complexity (Zerial and McBride, 2001). The human genome contains more than 60 Rabs, while the genomes of the fruit fly, nematode and yeast have 26, 29 and 11 Rabs, respectively (Bock *et al.*, 2001). Some Rabs, e.g. Rab5 and Rab7, are ubiquitous (Stenmark and Olkkonen, 2001), while others, e.g. Rab3 (Schluter *et al.*, 2002) and Rab27A (Hume *et al.*, 2001; Stinchcombe *et al.*, 2001), are unique to particular cells, tissues, organs and species (Seabra *et al.*, 2002). Rab11 is one of the ubiquitous Rabs, distributed in the trans-Golgi network (TGN), post-Golgi vesicles and recycling endosomes (Urbe *et al.*, 1993; Ullrich *et al.*, 1996; Ren *et al.*, 1998; McNiven and Thompson, 2006). In Chinese hamster ovary (CHO) cells, Rab11 was shown to regulate the recycling of the transferrin receptor to the plasma membrane (Ullrich *et al.*, 1996; Ren *et al.*, 1998). In parietal epithelial cells, Rab11 was also shown to control the cell surface expression of H^+/K^+ ATPase by regulating recycling to the plasma membrane (Goldenring *et al.*, 1994). Rab11 was also implicated in the transport from the Golgi apparatus to plasma membrane (Chen *et al.*, 1999). In yeast, two Rab11 homologues, Ypt31p and Ypt32p, were assumed to regulate the secretory pathway as a *ypt31/ypt32*-mutant was unable to secrete invertase (Benli *et al.*, 1996). In addition to recycling and exocytosis, Rab11 regulates transport from early endosomes to TGN (Wilcke *et al.*, 2000), suggesting that it may interconnect the endocytic and secretory pathways (Somsel Rodman and Wandinger-Ness, 2000; Savina *et al.*, 2002; Fader *et al.*, 2005). In the protozoan parasite *Trypanosoma brucei*, Rab11 was shown to be developmentally regulated and involved in the recycling of

transferrin receptors (ESAG6 and 7) (Jeffries *et al.*, 2001). In a non-pathogenic soil-amoeba, *Dictyostelium discoideum*, Rab11 was found to be associated with and regulate the structure and functions of the contractile vacuole system (Harris *et al.*, 2001).

The enteric protozoan parasite *Entamoeba histolytica* is a causative agent of an estimated 50 million cases of amoebic dysentery, colitis and liver abscess in humans, which leads to 100 000 deaths annually (Stanley *et al.*, 1995). This unicellular protist has 91–105 Rab genes (Lal *et al.*, 2005; Saito-Nakano *et al.*, 2005) despite its small genome (20 Mb) (Loftus *et al.*, 2005) and a simple life cycle, consisting of only two developmental stages, the disease-causing trophozoites and the dormant cysts (Eichinger, 1997). Vesicular trafficking plays a critical role in the parasitic life style and virulence of *E. histolytica*. Developmental changes, i.e. encystation and excystation, which require drastic morphological and biochemical changes, are accompanied by a radical reorganization of organelles and the synthesis, sorting and degradation of a large number of proteins. In the intestinal lumen and the tissues, the trophozoites actively absorb nutrients by degrading endocytosed macromolecules and also by engulfing and degenerating phagocytosed microorganisms and host cells. In addition, to establish a microenvironment suitable for colonization, they secrete various hydrolytic and membranolytic factors including cysteine proteases (Que and Reed, 2000) and the pore-forming peptide amoebapore (Leippe, 1999). Cysteine proteases compose a family of 44 members (Tillack *et al.*, 2006), and are currently considered primarily responsible for the pathogenesis. CP1 and CP5 were shown to be absent or degenerated in a closely related but non-pathogenic *Entamoeba dispar* species (Bruchhaus *et al.*, 1996; Willhoeft *et al.*, 1999). Overexpression of CP2 caused an augmentation of the destruction of cell monolayers, but no change in the formation of abscesses in the liver (Hellberg *et al.*, 2001). Antisense inhibition of CP5 resulted in a reduced capacity of liver abscess formation (Ankri *et al.*, 1999) and a reduced production of the inflammatory cytokines interleukin 1β and interleukin 8 by intestinal epithelial cells (Zhang *et al.*, 2000). It was also shown that in patients with invasive amoebiasis, there is a correlation among the levels of extracellular cysteine protease, epithelial damage and production of anticysteine protease antibodies (Reed *et al.*, 1989).

Although an understanding of the biosynthesis and transport of cysteine proteases is essential for comprehending the virulence of this parasite and also for the development of measures to intervene in its transmission, the molecular mechanisms of cysteine protease transport have only started to be unveiled (Temesvari *et al.*, 1999; McGugan and Temesvari, 2003; Saito-Nakano *et al.*, 2004; 2007; Nakada-Tsukui *et al.*, 2005; Saric *et al.*, 2006; Sato *et al.*, 2006). It was previously shown that cysteine proteases were abundant in the early and late endosomes, and colocalized with *Eh*Rab7A and *Eh*Rab11A, suggesting these Rabs to be involved in their transport (Temesvari *et al.*, 1999). We previously showed that the transport of cysteine proteases during phagocytosis is regulated by *Eh*Rab5 and *Eh*Rab7A (Saito-Nakano *et al.*, 2004; Nakada-Tsukui *et al.*, 2005). These two Rabs are involved in the formation of an unique preparatory compartment, the 'prephagosomal vacuole', which likely serves as a site for the processing, activation and temporary storage of cysteine proteases targeted at phagosomes. We also showed that the targeting of cysteine proteases is mediated by *Eh*Rab7A, and the interaction of *Eh*Rab7A with the retromer-like complex indirectly controls the efficiency with which cysteine proteases are transported to lysosomes. Furthermore, we have recently shown that the transport of cysteine proteases to lysosome was regulated by another member of Rab7 isotypes, *Eh*Rab7B (Saito-Nakano *et al.*, 2007). However, the expression of neither wild type nor mutant forms of *Eh*Rab5, *Eh*Rab7A and *Eh*Rab7B resulted in drastic changes in transport, suggesting the presence of other Rab(s) that play a crucial role in the process.

E. histolytica possesses four Rab11 homologues, *Eh*Rab11A (Temesvari *et al.*, 1999; McGugan and Temesvari, 2003), *Eh*Rab11B, *Eh*Rab11C (Saito-Nakano *et al.*, 2001; 2005) and *Eh*Rab11D (Saito-Nakano *et al.*, 2005), which show 55–63% mutual identity (Saito-Nakano *et al.*, 2005). It has been suggested that *Eh*Rab11A plays a role in the transport during starvation and encystation as it is concentrated at the periphery of the cell under these conditions (McGugan and Temesvari, 2003). In this study, we characterized the second member of the Rab11 gene family, *Eh*Rab11B. We showed that *Eh*Rab11B plays a pivotal role in the transport and secretion of the major cysteine proteases, and cytolytic activity against mammalian cells.

Results

Expression of EhRab11 isotypes measured by quantitative real-time (RT) polymerase chain reaction (PCR)

In order to see relative levels of the mRNA of Rab11 isotypes in *E. histolytica*, the amounts of a steady state transcript of *Eh*Rab11A-D, as well as *Eh*Rab5 and *Eh*Rab7A, in the trophozoite stage were measured by quantitative RT-PCR with RNA polymerase II 15 kDa subunit as an internal control (Fig. 1). The relative mRNA level of *Eh*Rab11B was approximately 67–74% that of *Eh*Rab11A and *Eh*Rab7A, and significantly higher than levels of the other two *Eh*Rab11 isotypes (*Eh*Rab11C and *Eh*Rab11D) and *Eh*Rab5.

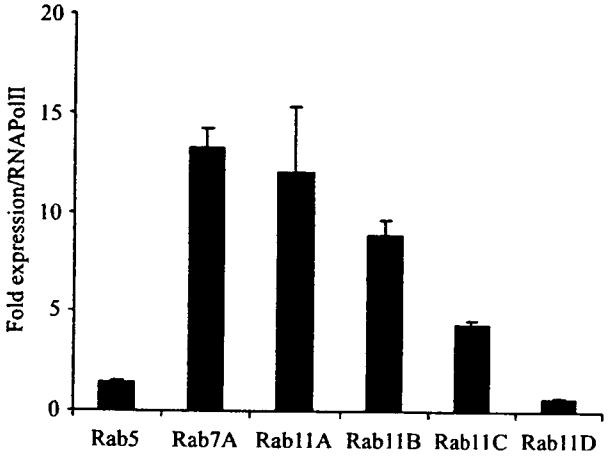

Fig. 1. Relative expression of *Eh*Rab11 in *E. histolytica*. Trophozoites in the logarithmic growth phase were harvested for the extraction of total RNA and synthesis of cDNA. The RT-PCR was performed as described in *Experimental procedures*, and the expression levels are shown relative to the amount of RNA polymerase. Error bars represent the standard error of the mean of three independent experiments.

Subcellular distribution of EhRab11B

Rab GTPases perform their respective functions in confined intracellular compartments. To understand the different functions of Rab11 isotypes in *E. histolytica*, we first examined the intracellular distribution of *Eh*Rab11B using the amoebic transformant that expressed HA-tagged *Eh*Rab11B. HA-tagged *Eh*Rab11B appeared to be associated with membranes or dot-like structures scattered throughout the cytosol. When the transformant was incubated with the fluid-phase marker FITC-dextran for 10 or 30 min and subjected to an immunofluorescence assay using anti-HA antibody, no vesicle/vacuole was simultaneously labelled with both FITC-dextran and anti-HA antibody (data not shown). Next, the HA-*Eh*Rab11B transformant was incubated with FITC-dextran for 60 min and then chased in a marker-free medium for 120 min. We observed a partial colocalization of FITC-dextran and *Eh*Rab11B (Fig. 2). We quantified the colocalization with two parameters: the percentage of trophozoites that contained FITC-dextran- and *Eh*Rab11B double-positive vesicles/vacuoles and the percentage of FITC-dextran- and *Eh*Rab11B double-positive vesicles/vacuoles among FITC-dextran-labelled vesicles/vacuoles. These two parameters showed similar kinetics; they gradually increased up to 60 min of chase, and then decreased at 120 min (Fig. 2B and C). We verified the localization and kinetics of *Eh*Rab11B during endocytosis using the wild-type strain and antibody raised against the recombinant *Eh*Rab11B to obtain comparable results (data not shown). We stained the *Eh*Rab11B transformant with LysoTracker Red, and rarely found the colocalization of *Eh*Rab11B and the acidic compartment labelled with LysoTracker (data not shown). We also carried out an immunofluorescence assay using a transformant that expressed CP5 with a HA-tag at the carboxyl terminus (Sato *et al.*, 2006) and anti-HA and anti-*Eh*Rab11B antibodies (Fig. 3A). We observed a partial colocalization of epitope-tagged CP5 and endogenous *Eh*Rab11B. The HA-*Eh*Rab11B-expressing transformant was also stained with antibody against the Sec61 α-subunit and dolicol-*P*-mannose synthase (DPMS), markers for the endoplasmic reticulum, showing no apparent colocalization with *Eh*Rab11B (Fig. 3B and C).

We further investigated if *Eh*Rab11B is involved in the transport to and/or maturation of lysosomes. We examined the acidity of whole amoebae by measuring the fluorescence intensity of the LysoTracker-stained acidic compartment of the *Eh*Rab11B-overexpressing and control transformants in a FACS-based analysis. We found no difference in the volume of the acidic compartment between these two transformants (data not shown). The results suggest that *Eh*Rab11B is not primarily associated with either late endosomes or lysosomes but confined to a compartment that only partially overlaps the endocytic and/or recycling pathway.

Overexpression of EhRab11B was accompanied by a dramatic increase of cysteine protease activity

It has been well established that secreted cysteine proteases play an indispensable role in amoebic invasion and tissue destruction due to their hydrolytic and degradative activities towards extracellular matrix proteins (Stanley *et al.*, 1995). We investigated the effects of the overexpression of *Eh*Rab11B on the secretion of cysteine proteases. We first examined the degree of overexpression (i.e. fold increase) in the HA-*Eh*Rab11B transformant compared with the control transformant (Fig. 4A). We estimated that the *Eh*Rab11B protein level increased by approximately ninefold as estimated from quantification of fluorescent signals by chemiluminescence detection with immunoblots obtained using anti-*Eh*Rab11B antibody (data not shown).

We examined cysteine protease activity in the lysate and culture supernatant of the HA-*Eh*Rab11B-overexpressing transformant, by measuring hydrolysis of the synthetic peptide substrate, z-Arg-Arg-7-amino-4-trifluoromethylcoumarin (Fig. 4B and C). It has been well established that the amoebic cysteine proteases have a strong preference for peptides containing Arg residues at the P1 and P2 positions (Jacobs *et al.*, 1998). Cysteine protease activity was 15-fold higher in the culture supernatant of the *Eh*Rab11B-overexpressing transformant than that of the control transformant ($P < 0.001$; Fig. 4C). Similarly, the total cysteine protease activity in the lysate of the *Eh*Rab11B-overexpressing transformant was 2.6-fold the control level ($P < 0.005$; Fig. 4B). The observed protease

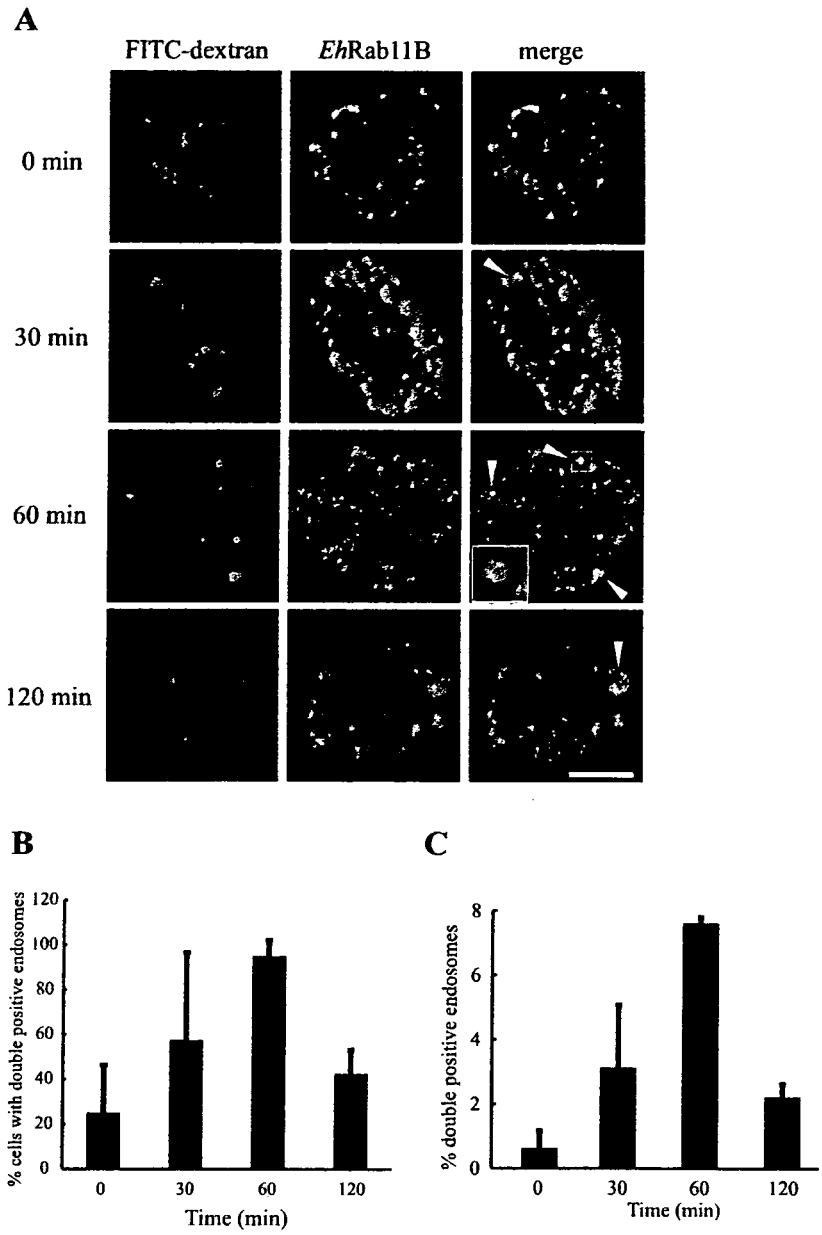

Fig. 2. Colocalization of *Eh*Rab11B and the fluid-phase marker.
A. The amoebae were pulsed with FITC-dextran for 1 h and further chased for the periods indicated (0, 30, 60 and 120 min). Images of immunofluorescence using anti-HA antibody to probe 3HA-tagged *Eh*Rab11B (red) together with FITC-dextran (green) are shown. White arrowheads indicate endocytosed FITC-dextran colocalized with *Eh*Rab11B. The islet shows a magnified image. Bar, 10 μm.
B. The percentage of trophozoites containing at least one FITC-dextran/*Eh*Rab11B double-positive vesicle/vacuole is shown.
C. The proportion of FITC-dextran/*Eh*Rab11B double-positive vesicles/vacuoles among all FITC-dextran-positive endosomes is shown. Error bars represent the standard error of the mean of two independent experiments.

activity was completely abolished when trophozoites were pretreated with 200 μM of E64, a potent, irreversible and highly selective cysteine protease inhibitor (Jacobs *et al.*, 1998; Que *et al.*, 2002) (data not shown).

To confirm these results and further determine which cysteine protease isotypes were over-produced and secreted, we performed gelatin substrate gel electrophoresis. The lysates (Fig. 4D) and culture-supernatant (Fig. 4E) of the *Eh*Rab11B-overexpressing and control transformants yielded zymograms of three predominant bands of cysteine protease activity in the range of 29–60 kDa on SDS-PAGE under non-reducing conditions, likely corresponding to CP1, 2 and 5, consistent with previous findings (Hellberg *et al.*, 2000). Although the ratio of the three major cysteine protease bands could not be determined, all three bands in both the lysate and supernatant appeared more intense in the *Eh*Rab11B-overexpressing transformant than control transformant, with the intensity of the band corresponding to CP1 increasing most remarkably among the three cysteine proteases. All three bands were abolished when trophozoites were pretreated with 200 μM E64 (data not shown).

It has been recently shown that cysteine proteases are transported via the brefeldin A (BFA)-insensitive route inducible by external stimuli (Manning-Cela *et al.*, 2003). To see if the augmented secretion of cysteine proteases in

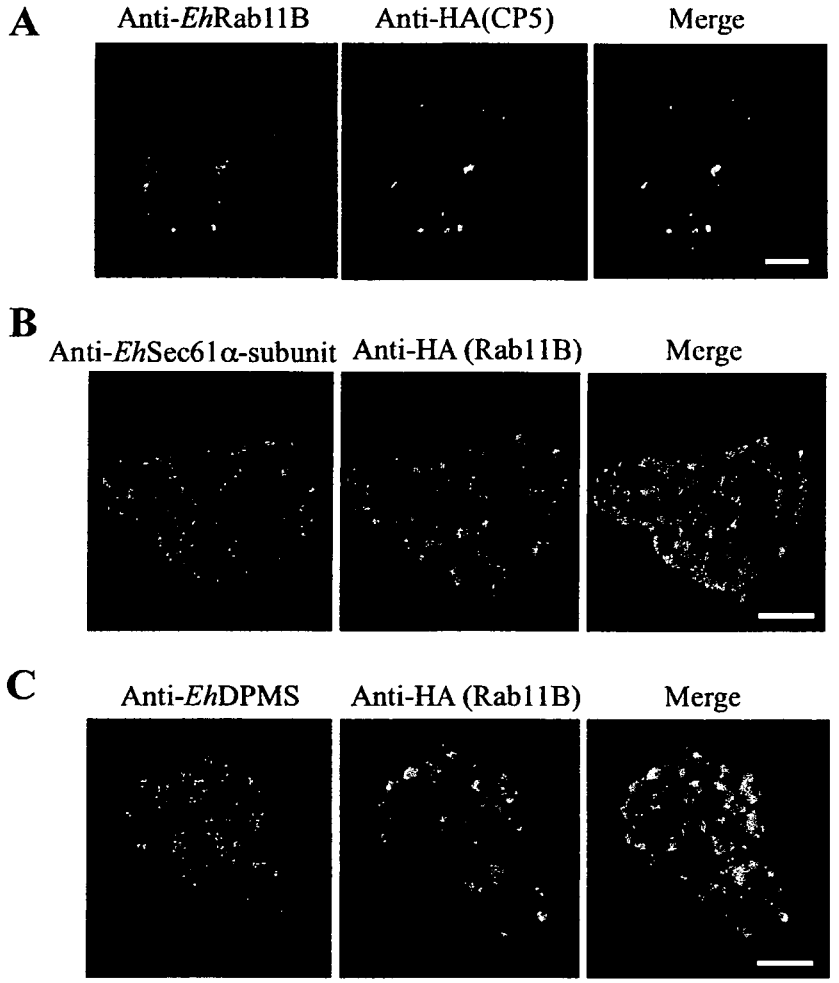

Fig. 3. *Eh*Rab11B is partially associated with CP5, and not associated with the endoplasmic reticulum.
A. Partial colocalization of *Eh*Rab11B and CP5. An immunofluorescence assay was conducted using a transformant that expressed CP5 with a HA-tag at the carboxyl terminus (Sato *et al.*, 2006) and anti-HA and anti-*Eh*Rab11B antibodies.
B and C. Lack of colocalization of *Eh*Rab11B and the markers for the endoplasmic reticulum. The *Eh*Rab11B-overexpressing transformant was stained with anti-*Eh*Sec61 α-subunit (B, green)or anti-*Eh*DPMS (C, green) and anti-HA antibody to visualize *Eh*Rab11B (red). Bars, 10 μm.

the *Eh*Rab11B-overexpressing transformant is due to the activation of the default BFA-insensitive pathway or alternative BFA-sensitive pathway(s), zymograms of the BFA-treated and untreated transformants were compared (Fig. 4F and G). The zymogram did not change with BFA treatment in either the *Eh*Rab11B-overexpressing or control transformant, suggesting that activation of the default BFA-insensitive pathway is likely the reason for the observed phenotype. The transport of the putative fibronectin receptor, detected with the monoclonal antibody against the galactose/N-acetylgalactosamine-specific lectin intermediate subunit (Cheng *et al.*, 2001) was partially inhibited under the same conditions (data not shown).

Overexpression of EhRab11B increased both intracellular and secreted amounts of three major cysteine proteases

To further examine the level of expression and secretion of individual cysteine proteases in the *Eh*Rab11B-overexpressing transformant, the relative amounts of three major cysteine proteases, i.e. CP1, CP2 and CP5, were determined by fluorometric estimation of immunoblots using specific antibodies raised against recombinant cysteine proteases (Sato *et al.*, 2006). These cysteine proteases were detected as a single 29-kDa band under reducing conditions (Fig. 5). We first verified the specificity (or cross-reactivity) of each antibody against the cysteine proteases (Fig. 5C). Despite high sequence homology among the three cysteine proteases (CP1 and CP2, 81%; CP1 and CP5, 51%; CP2 and CP5, 50%), anti-CP2 and anti-CP5 specifically reacted with the corresponding cysteine protease, while anti-CP1 antibody cross-reacted with CP2 with a similar efficiency to CP1. In the culture supernatant, the amount of CP1/CP2, CP2 and CP5, detected by anti-CP1, CP2 and CP5 antibody, respectively, increased by 18.0, 4.2 and 2.0-fold, respectively, in the *Eh*Rab11B-overexpressing transformant (Fig. 5B). Similarly, in the lysate, the amount increased by 6.6, 3.2 and 2.0-fold, respectively (Fig. 5A). These data were consistent with the results of cysteine protease activity described